3.10.5 Operational Classification

For the purpose of Article 3.10, the Owner or those having jurisdiction shall classify the bridge into one of three **operational** categories as follows:

- Critical bridges,
- Essential bridges, or
- Other bridges.

The basis of classification shall include social/survival and security/defense requirements. In classifying a bridge, consideration should be given to possible future changes in conditions and requirements.

C3.10.5

Essential bridges are generally those that should, as a minimum, be open to emergency vehicles and for security/defense purposes immediately after the design earthquake, i.e., a 1,000-year return period event. However, some bridges must remain open to all traffic after the design earthquake and be usable by emergency vehicles and for security/defense purposes immediately after a large earthquake, e.g., a 2,500-year return period event. These bridges should be regarded as critical structures.

3.10.6 Seismic Performance Zones

Each bridge shall be assigned to one of the four seismic zones in accordance with Table 1 using the value of S_{D1} given by Eq. 3.10.4.2-6.

C3.10.6

These seismic zones reflect the variation in seismic risk across the country and are used to permit different requirements for methods of analysis, minimum support lengths, column design details, and foundation and abutment design procedures.

Table 3.10.6-1 Seismic Zones.

Acceleration Coefficient, S_{D1}	Seismic Zone
$S_{D1} \le 0.15$	1
$0.15 < S_{D1} \le 0.30$	2
$0.30 < S_{D1} \le 0.50$	3
$0.50 < S_{D1}$	4

3.10.7 Response Modification Factors

3.10.7.1 General

To apply the response modification factors specified herein, the structural details shall satisfy the provisions of Articles 5.10.2.2, 5.10.11, and 5.13.4.6.

Except as noted herein, seismic design force effects for substructures and the connections between parts of structures, listed in Table 2, shall be determined by dividing the force effects resulting from elastic analysis by the appropriate response modification factor, R, as specified in Tables 1 and 2, respectively.

As an alternative to the use of the R-factors, specified in Table 2 for connections, monolithic joints between structural members and/or structures, such as a column-to-footing connection, may be designed to transmit the maximum force effects that can be developed by the inelastic hinging of the column or multicolumn bent they connect as specified in Article 3.10.9.4.3.

If an inelastic time history method of analysis is used, the response modification factor, R, shall be taken as 1.0 for all substructure and connections.

C3.10.7.1

These Specifications recognize that it is uneconomical to design a bridge to resist large earthquakes elastically. Columns are assumed to deform inelastically where seismic forces exceed their design level, which is established by dividing the elastically computed force effects by the appropriate R-factor.

R-factors for connections are smaller than those for substructure members in order to preserve the integrity of the bridge under these extreme loads. For expansion joints within the superstructure and connections between the superstructure and abutment, the application of the R-factor results in force effect magnification. Connections that transfer forces from one part of a structure to another include, but are not limited to, fixed bearings, expansion bearings with either restrainers, STUs, or dampers, and shear keys. For one-directional bearings, these R-factors are used in the restrained direction only. In general, forces determined on the basis of plastic hinging will be less than those given by using Table 2, resulting in a more economical design.

Table 3.10.7.1-1 Response Modification Factors—Substructures.

Substructure	**Operational** Category		
	Critical	Essential	Other
Wall-type piers—larger dimension	1.5	1.5	2.0
Reinforced concrete pile bents			
• Vertical piles only	1.5	2.0	3.0
• With batter piles	1.5	1.5	2.0
Single columns	1.5	2.0	3.0
Steel or composite steel and concrete pile bents			
• Vertical pile only	1.5	3.5	5.0
• With batter piles	1.5	2.0	3.0
Multiple column bents	1.5	3.5	5.0

Table 3.10.7.1-2 Response Modification Factors—Connections.

Connection	All **Operational** Categories
Superstructure to abutment	0.8
Expansion joints within a span of the superstructure	0.8
Columns, piers, or pile bents to cap beam or superstructure	1.0
Columns or piers to foundations	1.0

3.10.7.2 Application

Seismic loads shall be assumed to act in any lateral direction.

The appropriate R-factor shall be used for both orthogonal axes of the substructure.

A wall-type concrete pier may be analyzed as a single column in the weak direction if all the provisions for columns, as specified in Section 5, are satisfied.

C3.10.7.2

Usually the orthogonal axes will be the longitudinal and transverse axes of the bridge. In the case of a curved bridge, the longitudinal axis may be the chord joining the two abutments.

Wall-type piers may be treated as wide columns in the strong direction, provided the appropriate R-factor in this direction is used.

In lieu of restrainers, STUs may be used and designed for either the elastic force calculated in Article 4.7 or the maximum force effects generated by inelastic hinging of the substructure as specified in Article 3.10.7.1.

3.10.9.6 Hold-Down Devices

For Seismic Zones 2, 3, and 4, hold-down devices shall be provided at supports and at hinges in continuous structures where the vertical seismic force due to the longitudinal seismic load opposes and exceeds 50 percent, but is less than 100 percent, of the reaction due to permanent loads. In this case, the net uplift force for the design of the hold-down device shall be taken as 10 percent of the reaction due to permanent loads that would be exerted if the span were simply supported.

If the vertical seismic forces result in net uplift, the hold-down device shall be designed to resist the larger of either:

- 120 percent of the difference between the vertical seismic force and the reaction due to permanent loads, or
- 10 percent of the reaction due to permanent loads.

3.10.10 Requirements for Temporary Bridges and Stage Construction

Any bridge or partially constructed bridge that is expected to be temporary for more than five years shall be designed using the requirements for permanent structures and shall not use the provisions of this Article.

The requirement that an earthquake shall not cause collapse of all or part of a bridge, as stated in Article 3.10.1, shall apply to temporary bridges expected to carry traffic. It shall also apply to those bridges that are constructed in stages and expected to carry traffic and/or pass over routes that carry traffic. The acceleration coefficient given in Article 3.10.2 may be reduced by a factor of not more than 2 in order to calculate the component elastic forces and displacements. Acceleration coefficients for construction sites that are close to active faults shall be the subject of special study. The response modification factors given in Article 3.10.7 may be increased by a factor of not more than 1.5 in order to calculate the design forces. This factor shall not be applied to connections as defined in Table 3.10.7.1-2.

The minimum seat width provisions of Article 4.7.4.4 shall apply to all temporary bridges and staged construction.

C3.10.10

The option to use a reduced acceleration coefficient is provided to reflect the limited exposure period.

3.11 EARTH PRESSURE: *EH*, *ES*, *LS*, AND *DD*

3.11.1 General

Earth pressure shall be considered as a function of the:

- Type and unit weight of earth,
- Water content,
- Soil creep characteristics,
- Degree of compaction,
- Location of groundwater table,
- Earth-structure interaction,
- Amount of surcharge,
- Earthquake effects,
- Back slope angle, and
- Wall inclination.

Silt and lean clay shall not be used for backfill unless suitable design procedures are followed and construction control measures are incorporated in the construction documents to account for their presence. Consideration shall be given for the development of pore water pressure within the soil mass in accordance with Article 3.11.3. Appropriate drainage provisions shall be provided to prevent hydrostatic and seepage forces from developing behind the wall in accordance with the provisions in Section 11. In no case shall highly plastic clay be used for backfill.

C3.11.1

Walls that can tolerate little or no movement should be designed for at-rest earth pressure. Walls which can move away from the soil mass should be designed for pressures between active and at-rest conditions, depending on the magnitude of the tolerable movements. Movement required to reach the minimum active pressure or the maximum passive pressure is a function of the wall height and the soil type. Some typical values of these mobilizing movements, relative to wall height, are given in Table C1, where:

Δ = movement of top of wall required to reach minimum active or maximum passive pressure by tilting or lateral translation (ft.)

H = height of wall (ft.)

Table C3.11.1-1 Approximate Values of Relative Movements Required to Reach Active or Passive Earth Pressure Conditions (*Clough and Duncan 1991*).

Type of Backfill	Values of Δ/H	
	Active	Passive
Dense sand	0.001	0.01
Medium dense sand	0.002	0.02
Loose sand	0.004	0.04
Compacted silt	0.002	0.02
Compacted lean clay	0.010	0.05
Compacted fat clay	0.010	0.05

The evaluation of the stress induced by cohesive soils is highly uncertain due to their sensitivity to shrink-swell, wet-dry and degree of saturation. Tension cracks can form, which considerably alter the assumptions for the estimation of stress. Extreme caution is advised in the determination of lateral earth pressures assuming the most unfavorable conditions. If possible, cohesive or other fine-grained soils should be avoided as backfill.

For walls retaining cohesive materials, the effects of soil creep should be taken into consideration in estimating the design earth pressures. Evaluation of soil creep is complex and requires duplication in the laboratory of the stress conditions in the field as discussed by Mitchell (*1976*).

Under stress conditions close to the minimum active or maximum passive earth pressures, cohesive soils indicated in Table C1 creep continually, and the movements shown produce active or passive pressures only temporarily. If there is no further movement, active pressures will increase with time, approaching the at-rest pressure, and passive pressures will decrease with time, approaching values on the order of 40 percent of the maximum short-term value. A conservative assumption to account for unknowns would be to use the at-rest pressure based on the residual strength of the soil.

3.11.2 Compaction

Where activity by mechanical compaction equipment is anticipated within a distance of one-half the height of the wall, taken as the difference in elevation between the point where finished grade intersects the back of the wall and the base of the wall, the effect of additional earth pressure that may be induced by compaction shall be taken into account.

C3.11.2

Compaction-induced earth pressures may be estimated using the procedures described by Clough and Duncan (*1991*). The heavier the equipment used to compact the backfill, and the closer it operates to the wall, the larger are the compaction-induced pressures. The magnitude of the earth pressures exerted on a wall by compacted backfill can be minimized by using only small rollers or hand compactors within a distance of one-half wall height from the back of the wall. For MSE structures, compaction stresses are already included in the design model and specified compaction procedures.

3.11.3 Presence of Water

If the retained earth is not allowed to drain, the effect of hydrostatic water pressure shall be added to that of earth pressure.

In cases where water is expected to pond behind a wall, the wall shall be designed to withstand the hydrostatic water pressure plus the earth pressure.

Submerged unit weights of the soil shall be used to determine the lateral earth pressure below the groundwater table.

C3.11.3

The effect of additional pressure caused by groundwater is shown in Figure C1.

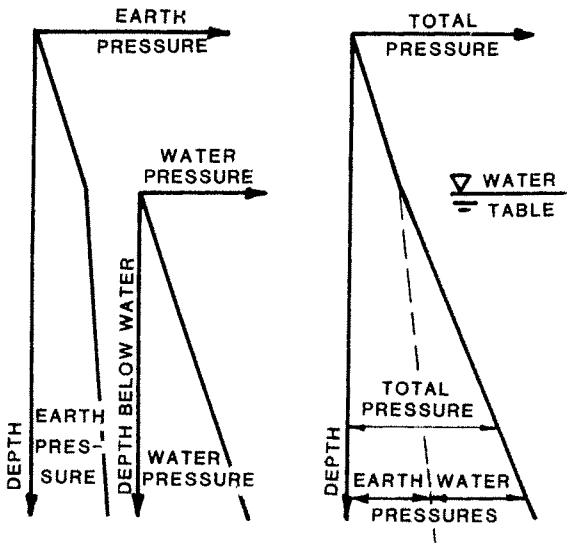

Figure C3.11.3-1 Effect of Groundwater Table.

The development of hydrostatic water pressure on walls should be eliminated through use of crushed rock, pipe drains, gravel drains, perforated drains or geosynthetic drains.

If the groundwater levels differ on opposite sides of the wall, the effects of seepage on wall stability and the potential for piping shall be considered. Pore water pressures shall be added to the effective horizontal stresses in determining total lateral earth pressures on the wall.

Pore water pressures behind the wall may be approximated by flow net procedures or various analytical methods.

3.11.4 Effect of Earthquake

The effects of wall inertia and probable amplification of active earth pressure and/or mobilization of passive earth masses by earthquake shall be considered.

C3.11.4

The Mononobe-Okabe method for determining equivalent static fluid pressures for seismic loads on gravity and semigravity retaining walls is presented in the appendix to Section 11.

The Mononobe-Okabe analysis is based, in part, on the assumption that the backfill soils are unsaturated and thus, not susceptible to liquefaction.

Where soils are subject to both saturation and seismic or other cyclic/instantaneous loads, special consideration should be given to address the possibility of soil liquefaction.

3.11.5 Earth Pressure: *EH*

3.11.5.1 Lateral Earth Pressure

C3.11.5.1

Lateral earth pressure shall be assumed to be linearly proportional to the depth of earth and taken as:

$$p = k\gamma_s z \qquad (3.11.5.1\text{-}1)$$

where:

p = lateral earth pressure (ksf)

k = coefficient of lateral earth pressure taken as k_o, specified in Article 3.11.5.2, for walls that do not deflect or move, k_a, specified in Articles 3.11.5.3, 3.11.5.6 and 3.11.5.7, for walls that deflect or move sufficiently to reach minimum active conditions, or k_p, specified in Article 3.11.5.4, for walls that deflect or move sufficiently to reach a passive condition

γ_s = unit weight of soil (kcf)

z = depth below the surface of earth (ft.)

The resultant lateral earth load due to the weight of the backfill shall be assumed to act at a height of $H/3$ above the base of the wall, where H is the total wall height, measured from the surface of the ground at the back of the wall to the bottom of the footing or the top of the leveling pad (for MSE walls).

Although previous versions of these Specifications have required design of conventional gravity walls for a resultant earth pressure located $0.4H$ above the wall base, the current specifications require design for a resultant located $H/3$ above the base. This requirement is consistent with historical practice and with calibrated resistance factors in Section 11. The resultant lateral load due to the earth pressure may act as high as $0.4H$ above the base of the wall for a mass concrete gravity retaining wall, where H is the total wall height measured from the top of the backfill to the base of the footing, where the wall deflects laterally, i.e., translates, in response to lateral earth loading. For such structures, the backfill behind the wall must slide down along the back of the wall for the retained soil mass to achieve the active state of stress. Experimental results indicate that the backfill arches against the upper portion of the wall as the wall translates, causing an upward shift in the location at which the resultant of the lateral earth load is transferred to the wall (*Terzaghi 1934; Clausen and Johansen et al. 1972; Sherif et al. 1982*). Such walls are not representative of typical gravity walls used in highway applications.

For most gravity walls which are representative of those used in highway construction, nongravity cantilever retaining walls or other flexible walls which tilt or deform laterally in response to lateral loading, e.g., MSE walls, as well as walls which cannot translate or tilt, e.g., integral abutment walls, significant arching of the backfill against the wall does not occur, and the resultant lateral load due to earth pressure acts at a height of $H/3$ above the base of the wall. Furthermore, where wall friction is not considered in the analysis, it is sufficiently conservative to use a resultant location of $H/3$ even if the wall can translate.

3.11.5.2 At-Rest Lateral Earth Pressure Coefficient, k_o

For normally consolidated soils, vertical wall, and level ground, the coefficient of at-rest lateral earth pressure may be taken as:

$$k_o = 1 - \sin \phi'_f \qquad (3.11.5.2\text{-}1)$$

where:

ϕ'_f = effective friction angle of soil

k_o = coefficient of at-rest lateral earth pressure

For overconsolidated soils, the coefficient of at-rest lateral earth pressure may be assumed to vary as a function of the overconsolidation ratio or stress history, and may be taken as:

C3.11.5.2

For typical cantilevered walls over 5.0 ft. high with structural grade backfill, calculations indicate that the horizontal movement of the top of the wall due to a combination of structural deformation of the stem and rotation of the foundation is sufficient to develop active conditions.

In many instances, the OCR may not be known with enough accuracy to calculate k_o using Eq. 2. Based on information on this issue provided by Holtz and Kovacs (*1981*), in general, for lightly overconsolidated sands ($OCR = 1$ to 2), k_o is in the range of 0.4 to 0.6. For highly overconsolidated sand, k_o can be on the order of 1.0.

$$k_o = (1 - \sin\phi'_f)(OCR)^{\sin\phi'_f} \qquad (3.11.5.2\text{-}2)$$

where:

OCR = overconsolidation ratio

Silt and lean clay shall not be used for backfill unless suitable design procedures are followed and construction control measures are incorporated in the construction documents to account for their presence. Consideration must be given for the development of pore water pressure within the soil mass in accordance with Article 3.11.3. Appropriate drainage provisions shall be provided to prevent hydrostatic and seepage forces from developing behind the wall in accordance with the provisions of Section 11. In no case shall highly plastic clay be used for backfill.

3.11.5.3 Active Lateral Earth Pressure Coefficient, k_a

Values for the coefficient of active lateral earth pressure may be taken as:

$$k_a = \frac{\sin^2(\theta + \phi'_f)}{\Gamma[\sin^2\theta \sin(\theta - \delta)]} \qquad (3.11.5.3\text{-}1)$$

in which:

$$\Gamma = \left[1 + \sqrt{\frac{\sin(\phi'_f + \delta)\sin(\phi'_f - \beta)}{\sin(\theta - \delta)\sin(\theta + \beta)}}\right]^2 \qquad (3.11.5.3\text{-}2)$$

where:

δ = friction angle between fill and wall taken as specified in Table 1 (°)

β = angle of fill to the horizontal as shown in Figure 1 (°)

θ = angle of back face of wall to the horizontal as shown in Figure 1 (°)

ϕ'_f = effective angle of internal friction (°)

For conditions that deviate from those described in Figure 1, the active pressure may be calculated by using a trial procedure based on wedge theory using the Culmann method (e.g., see *Terzaghi et al. 1996*).

The evaluation of the stress induced by cohesive soils is highly uncertain due to their sensitivity to shrink-swell, wet-dry and degree of saturation. Tension cracks can form, which considerably alter the assumptions for the estimation of stress. Extreme caution is advised in the determination of lateral earth pressures assuming the most unfavorable conditions. See Article C3.11.1 for additional guidance on estimating earth pressures in fine-grained soils. If possible, cohesive or other fine-grained soils should be avoided as backfill.

C3.11.5.3

The values of k_a by Eq. 1 are based on the Coulomb earth pressure theories. The Coulomb theory is necessary for design of retaining walls for which the back face of the wall interferes with the development of the full sliding surfaces in the backfill soil assumed in Rankine theory (Figure C1 and Article C3.11.5.8). Either Coulomb or Rankine wedge theory may be used for long healed cantilever walls shown in Figure C1a. In general, Coulomb wedge theory applies for gravity, semigravity and prefabricated modular walls with relatively steep back faces, and concrete cantilever walls with short heels.

For the cantilever wall in Figure C1b, the earth pressure is applied to a plane extending vertically up from the heel of the wall base, and the weight of soil to the left of the vertical plane is considered as part of the wall weight.

The differences between the Coulomb theory currently specified, and the Rankine theory specified in the past is illustrated in Figure C1. The Rankine theory is the basis of the equivalent fluid method of Article 3.11.5.5.

Silt and lean clay should not be used for backfill where free-draining granular materials are available. When using poorly draining silts or cohesive soils, extreme caution is advised in the determination of lateral earth pressures assuming the most unfavorable conditions. Consideration must be given for the development of pore water pressure within the soil mass in accordance with Article 3.11.3. Appropriate drainage provisions should be provided to prevent hydrostatic and seepage forces from developing behind the wall in accordance with the provisions in Section 11. In no case should highly plastic clay be used for backfill.

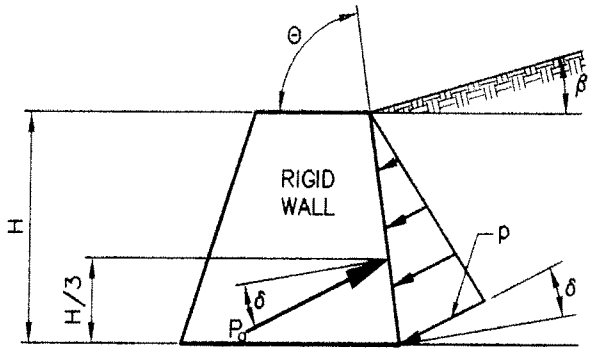

Figure 3.11.5.3-1 Notation for Coulomb Active Earth Pressure.

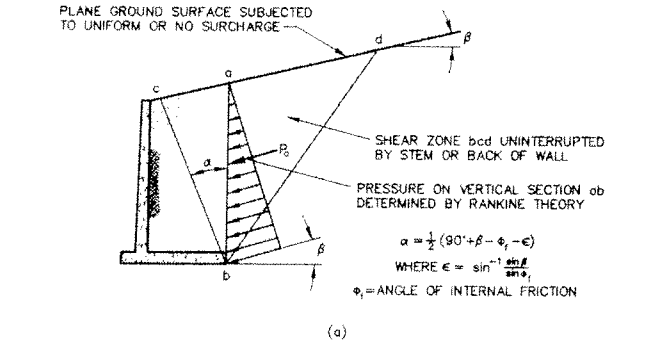

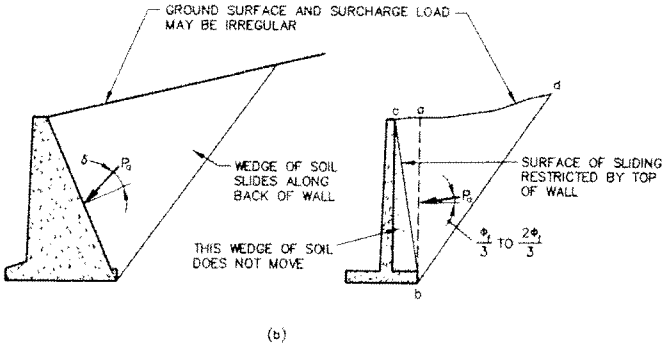

Figure C3.11.5.3-1 Application of (a) Rankine and (b) Coulomb Earth Pressure Theories in Retaining Wall Design.

Table 3.11.5.3-1 Friction Angle for Dissimilar Materials (*U.S. Department of the Navy 1982a*).

Interface Materials	Friction Angle, δ (°)	Coefficient of Friction, tan δ (dim.)
Mass concrete on the following foundation materials:		
• Clean sound rock	35	0.70
• Clean gravel, gravel-sand mixtures, coarse sand	29 to 31	0.55 to 0.60
• Clean fine to medium sand, silty medium to coarse sand, silty or clayey gravel	24 to 29	0.45 to 0.55
• Clean fine sand, silty or clayey fine to medium sand	19 to 24	0.34 to 0.45
• Fine sandy silt, nonplastic silt	17 to 19	0.31 to 0.34
• Very stiff and hard residual or preconsolidated clay	22 to 26	0.40 to 0.49
• Medium stiff and stiff clay and silty clay	17 to 19	0.31 to 0.34
Masonry on foundation materials has same friction factors.		
Steel sheet piles against the following soils:		
• Clean gravel, gravel-sand mixtures, well-graded rock fill with spalls	22	0.40
• Clean sand, silty sand-gravel mixture, single-size hard rock fill	17	0.31
• Silty sand, gravel or sand mixed with silt or clay	14	0.25
• Fine sandy silt, nonplastic silt	11	0.19
Formed or precast concrete or concrete sheet piling against the following soils:		
• Clean gravel, gravel-sand mixture, well-graded rock fill with spalls	22 to 26	0.40 to 0.49
• Clean sand, silty sand-gravel mixture, single-size hard rock fill	17 to 22	0.31 to 0.40
• Silty sand, gravel or sand mixed with silt or clay	17	0.31
• Fine sandy silt, nonplastic silt	14	0.25
Various structural materials:		
• Masonry on masonry, igneous and metamorphic rocks:		
○ dressed soft rock on dressed soft rock	35	0.70
○ dressed hard rock on dressed soft rock	33	0.65
○ dressed hard rock on dressed hard rock	29	0.55
• Masonry on wood in direction of cross grain	26	0.49
• Steel on steel at sheet pile interlocks	17	0.31

3.11.5.4 Passive Lateral Earth Pressure Coefficient, k_p

For noncohesive soils, values of the coefficient of passive lateral earth pressure may be taken from Figure 1 for the case of a sloping or vertical wall with a horizontal backfill or from Figure 2 for the case of a vertical wall and sloping backfill. For conditions that deviate from those described in Figures 1 and 2, the passive pressure may be calculated by using a trial procedure based on wedge theory, e.g., see Terzaghi et al. (*1996*). When wedge theory is used, the limiting value of the wall friction angle should not be taken larger than one-half the angle of internal friction, ϕ_f.

For cohesive soils, passive pressures may be estimated by:

C3.11.5.4

The movement required to mobilize passive pressure is approximately 10.0 times as large as the movement needed to induce earth pressure to the active values. The movement required to mobilize full passive pressure in loose sand is approximately 5 percent of the height of the face on which the passive pressure acts. For dense sand, the movement required to mobilize full passive pressure is smaller than 5 percent of the height of the face on which the passive pressure acts, and 5 percent represents a conservative estimate of the movement required to mobilize the full passive pressure. For poorly compacted cohesive soils, the movement required to mobilize full passive pressure is larger than 5 percent of the height of the face on which the pressure acts.

$$p_p = k_p \gamma_s z + 2c\sqrt{k_p} \qquad (3.11.5.4\text{-}1)$$

where:

p_p = passive lateral earth pressure (ksf)

γ_s = unit weight of soil (kcf)

z = depth below surface of soil (ft.)

c = soil cohesion (ksf)

k_p = coefficient of passive lateral earth pressure specified in Figures 1 and 2, as appropriate

Wedge solutions are inaccurate and unconservative for larger values of wall friction angle.

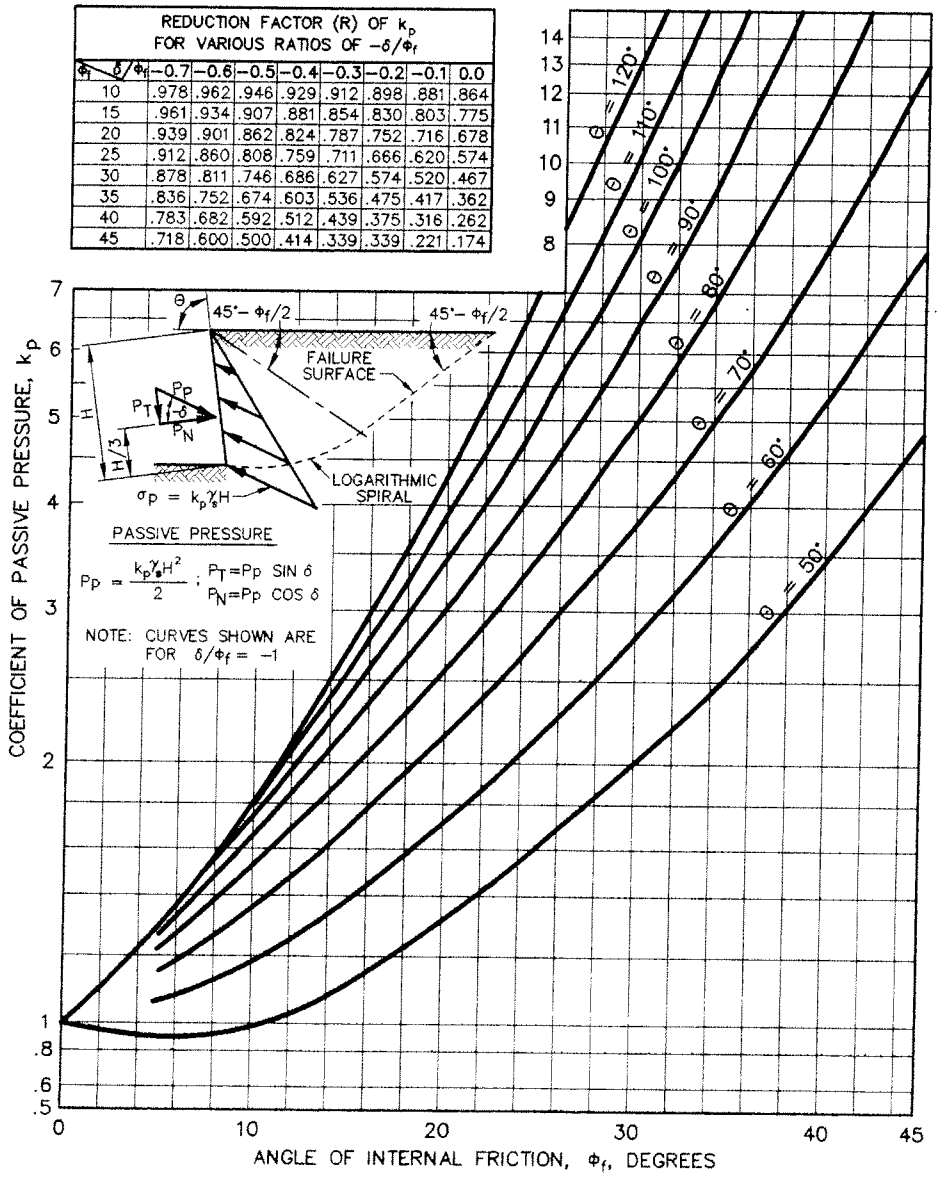

Figure 3.11.5.4-1 Computational Procedures for Passive Earth Pressures for Vertical and Sloping Walls with Horizontal Backfill (*U.S. Department of the Navy 1982a*).

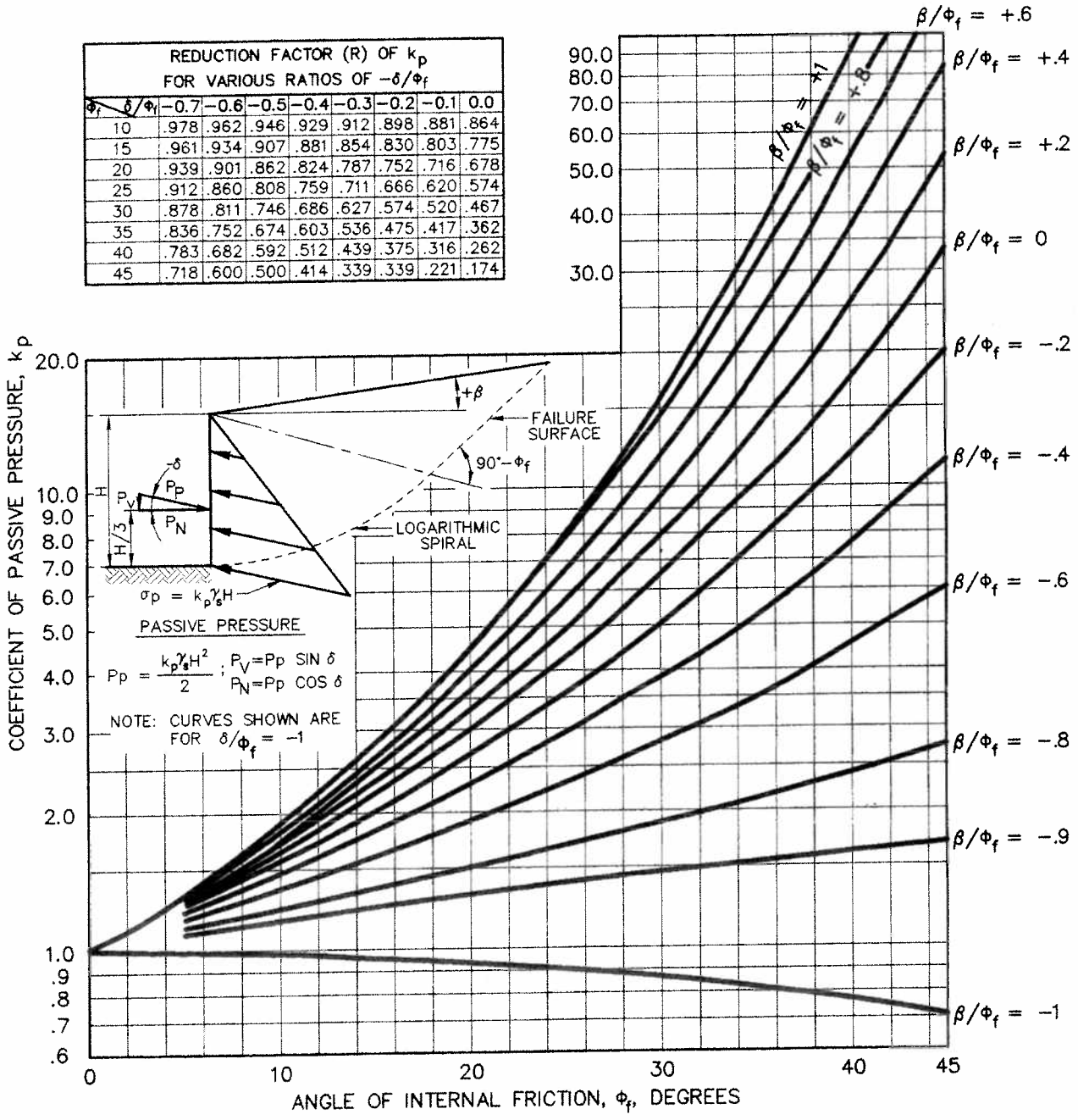

Figure 3.11.5.4-2 Computational Procedures for Passive Earth Pressures for Vertical Wall with Sloping Backfill (*U.S. Department of the Navy 1982a*).

3.11.5.5 Equivalent-Fluid Method of Estimating Rankine Lateral Earth Pressures

The equivalent-fluid method may be used where Rankine earth pressure theory is applicable.

The equivalent-fluid method shall only be used where the backfill is free-draining. If this criterion cannot be satisfied, the provisions of Articles 3.11.3, 3.11.5.1 and 3.11.5.3 shall be used to determine horizontal earth pressure.

C3.11.5.5

Applicability of Rankine theory is discussed in Article C3.11.5.3.

Values of the unit weights of equivalent fluids are given for walls that can tolerate very little or no movement as well as for walls that can move as much as 1.0 in. in 20.0 ft. The concepts of equivalent fluid unit weights have taken into account the effect of soil creep on walls.

Where the equivalent-fluid method is used, the basic earth pressure, p (ksf), may be taken as:

$$p = \gamma_{eq}\, z \qquad (3.11.5.5\text{-}1)$$

where:

γ_{eq} = equivalent fluid unit weight of soil, not less than 0.030 (kcf)

z = depth below surface of soil (ft.)

The resultant lateral earth load due to the weight of the backfill shall be assumed to act at a height of $H/3$ above the base of the wall, where H is the total wall height, measured from the surface of the ground to the bottom of the footing.

Typical values for equivalent fluid unit weights for design of a wall of height not exceeding 20.0 ft. may be taken from Table 1, where:

Δ = movement of top of wall required to reach minimum active or maximum passive pressure by tilting or lateral translation (ft.)

H = height of wall (ft.)

β = angle of fill to the horizontal (°)

The magnitude of the vertical component of the earth pressure resultant for the case of sloping backfill surface may be determined as:

$$P_v = P_h \tan\beta \qquad (3.11.5.5\text{-}2)$$

where:

$$P_h = 0.5\gamma_{eq} H^2 \qquad (3.11.5.5\text{-}3)$$

If the backfill qualifies as free-draining (i.e., granular material with < 5 percent passing a No. 200 sieve), water is prevented from creating hydrostatic pressure.

For discussion on the location of the resultant of the lateral earth force see Article C3.11.5.1.

The values of equivalent fluid unit weight presented in Table 1 for $\Delta/H = 1/240$ represent the horizontal component of active earth pressure based on Rankine earth pressure theory. This horizontal earth pressure is applicable for cantilever retaining walls for which the wall stem does not interfere with the sliding surface defining the Rankine failure wedge within the wall backfill (Figure C3.11.5.3-1). The horizontal pressure is applied to a vertical plane extending up from the heel of the wall base, and the weight of soil to the left of the vertical plane is included as part of the wall weight.

For the case of a sloping backfill surface in Table 1, a vertical component of earth pressure also acts on the vertical plane extending up from the heel of the wall.

Table 3.11.5.5-1 Typical Values for Equivalent Fluid Unit Weights of Soils.

Type of Soil	Level Backfill		Backfill with $\beta = 25°$	
	At-Rest γ_{eq} (kcf)	Active $\Delta/H = 1/240$ γ_{eq} (kcf)	At-Rest γ_{eq} (kcf)	Active $\Delta/H = 1/240$ γ_{eq} (kcf)
Loose sand or gravel	0.055	0.040	0.065	0.050
Medium dense sand or gravel	0.050	0.035	0.060	0.045
Dense sand or gravel	0.045	0.030	0.055	0.040

3.11.5.6 Lateral Earth Pressures for Nongravity Cantilevered Walls

For permanent walls, the simplified lateral earth pressure distributions shown in Figures 1 through 3 may be used. If walls will support or are supported by cohesive soils for temporary applications, walls may be designed based on total stress methods of analysis and undrained shear strength parameters. For this latter case, the simplified earth pressure distributions shown in Figures 4 through 7 may be used with the following restrictions:

- The ratio of total overburden pressure to undrained shear strength, N_s (see Article 3.11.5.7.2), should be < 3 at the wall base.
- The active earth pressure shall not be less than 0.25 times the effective overburden pressure at any depth, or 0.035 ksf/ft. of wall height, whichever is greater.

For temporary walls with discrete vertical elements embedded in granular soil or rock, Figures 1 and 2 may be used to determine passive resistance and Figures 4 and 5 may be used to determine the active earth pressure due to the retained soil.

Where discrete vertical wall elements are used for support, the width, b, of each vertical element shall be assumed to equal the width of the flange or diameter of the element for driven sections and the diameter of the concrete-filled hole for sections encased in concrete.

The magnitude of the sloping surcharge above the wall for the determination of P_{a2} in Figure 4 should be based on the wedge of soil above the wall within the active wedge.

In Figure 5, a portion of negative loading at top of wall due to cohesion is ignored and hydrostatic pressure in a tension crack should be considered, but is not shown on the figure.

C3.11.5.6

Nongravity cantilevered walls temporarily supporting or supported by cohesive soils are subject to excessive lateral deformation if the undrained soil shear strength is low compared to the shear stresses. Therefore, use of these walls should be limited to soils of adequate strength as represented by the stability number N_s (see Article 3.11.5.7.2).

Base movements in the soil in front of a wall become significant for values of N_s of about 3 to 4, and a base failure can occur when N_s exceeds about 5 to 6 (*Terzaghi and Peck 1967*).

In Figures 1, 2, 4 and 5, the width b of discrete vertical wall elements effective in mobilizing the passive resistance of the soil is based on a method of analysis by Broms (*1964a, 1964b*) for single vertical piles embedded in cohesive or cohesionless soil and assumes a vertical element. The effective width for passive resistance of three times the element width, $3b$, is due to the arching action in soil and side shear on resisting rock wedges. The maximum width of $3b$ can be used when material in which the vertical element is embedded does not contain discontinuities that would affect the failure geometry. This width should be reduced if planes or zones of weakness would prevent mobilization of resistance through this entire width, or if the passive resistance zones of adjacent elements overlap. If the element is embedded in soft clay having a stability number less than 3, soil arching will not occur and the actual width shall be used as the effective width for passive resistance. Where a vertical element is embedded in rock, i.e., Figure 2, the passive resistance of the rock is assumed to develop through the shear failure of a rock wedge equal in width to the vertical element, b, and defined by a plane extending upward from the base of the element at an angle of 45°. For the active zone behind the wall below the mudline or groundline in front of the wall, the active pressure is assumed to act over one vertical element width, b, in all cases.

The design grade is generally taken below finished grade to account for excavation during or after wall construction or other disturbance to the supporting soil during the service life of the wall.

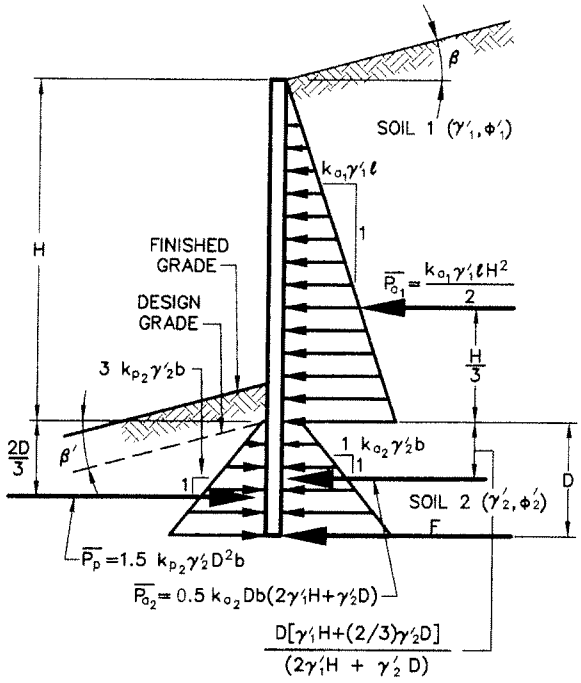

b = ACTUAL WIDTH OF EMBEDDED DISCRETE VERTICAL WALL ELEMENT BELOW DESIGN GRADE IN PLANE OF WALL (FT.).

Figure 3.11.5.6-1 Unfactored Simplified Earth Pressure Distributions for Permanent Nongravity Cantilevered Walls with Discrete Vertical Wall Elements Embedded in Granular Soil.

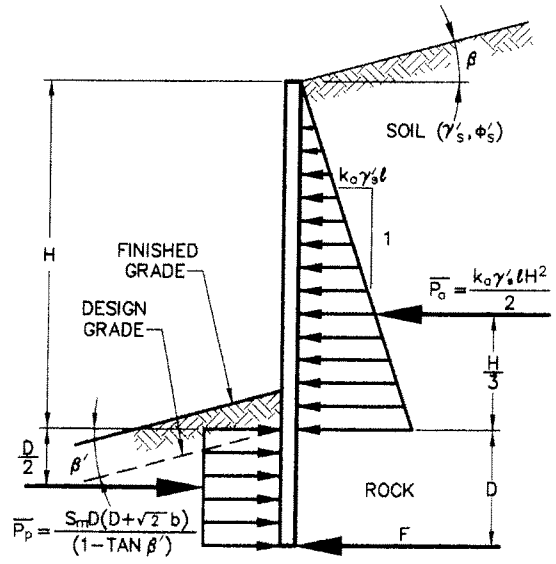

b = ACTUAL WIDTH OF EMBEDDED DISCRETE VERTICAL WALL ELEMENT BELOW DESIGN GRADE IN PLANE OF WALL (FT.).

Figure 3.11.5.6-2 Unfactored Simplified Earth Pressure Distributions for Permanent Nongravity Cantilevered Walls with Discrete Vertical Wall Elements Embedded in Rock.

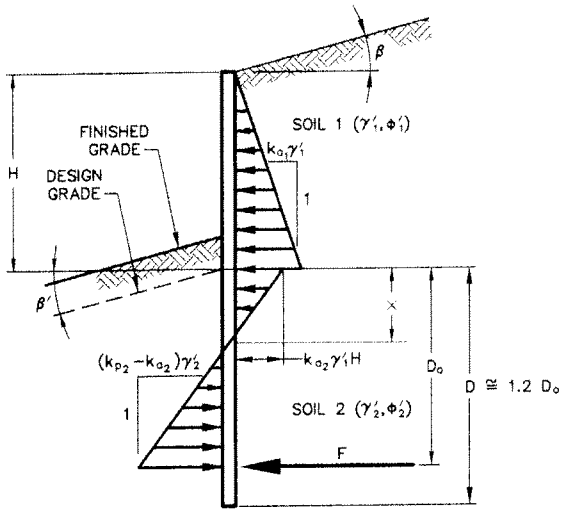

Figure 3.11.5.6-3 Unfactored Simplified Earth Pressure Distributions for Permanent Nongravity Cantilevered Walls with Continuous Vertical Wall Elements Embedded in Granular Soil Modified After Teng (*1962*).

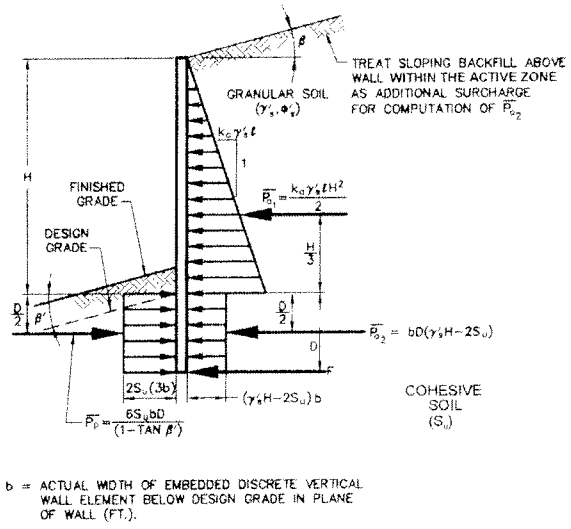

b = ACTUAL WIDTH OF EMBEDDED DISCRETE VERTICAL WALL ELEMENT BELOW DESIGN GRADE IN PLANE OF WALL (FT.).

Figure 3.11.5.6-4 Unfactored Simplified Earth Pressure Distributions for Temporary Nongravity Cantilevered Walls with Discrete Vertical Wall Elements Embedded in Cohesive Soil and Retaining Granular Soil.

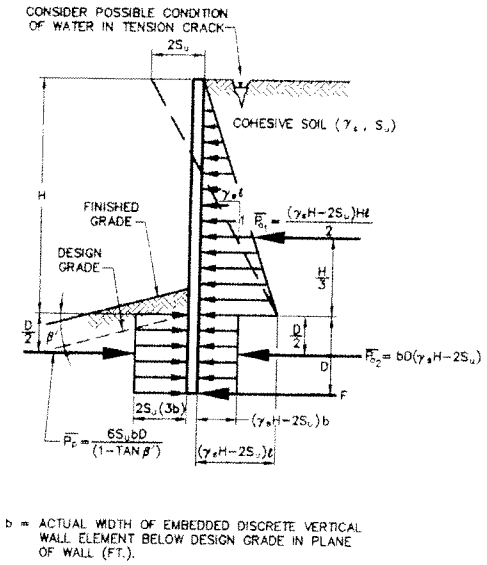

b = ACTUAL WIDTH OF EMBEDDED DISCRETE VERTICAL WALL ELEMENT BELOW DESIGN GRADE IN PLANE OF WALL (FT.).

Figure 3.11.5.6-5 Unfactored Simplified Earth Pressure Distributions for Temporary Nongravity Cantilevered Walls with Discrete Vertical Wall Elements Embedded in Cohesive Soil and Retaining Cohesive Soil.

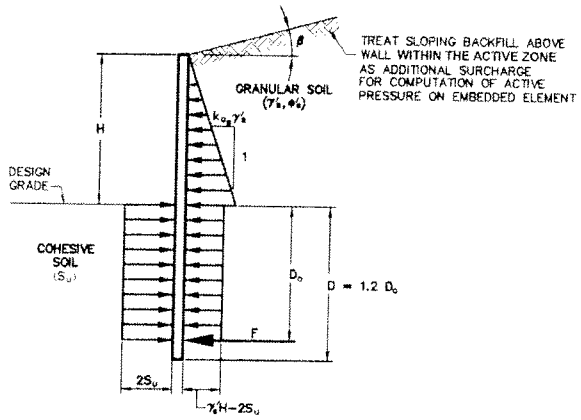

NOTE: FOR WALLS EMBEDDED IN GRANULAR SOIL, REFER TO FIGURE 3.11.5.6-3 AND USE FIGURE 3.11.5.6-7 FOR RETAINED COHESIVE SOIL WHEN APPROPRIATE.

Figure 3.11.5.6-6 Unfactored Simplified Earth Pressure Distributions for Temporary Nongravity Cantilevered Walls with Continuous Vertical Wall Elements Embedded in Cohesive Soil and Retaining Granular Soil Modified After Teng *(1962)*.

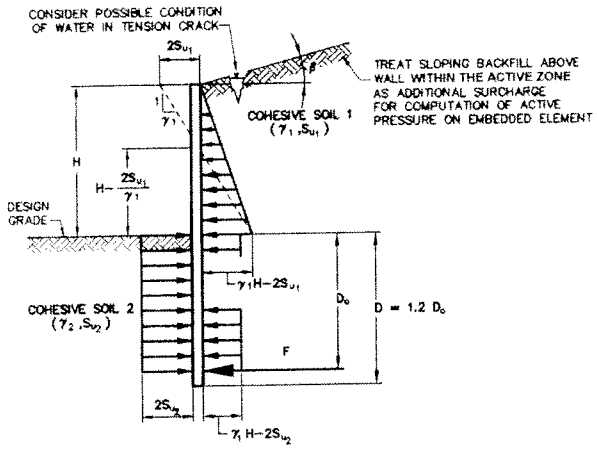

Figure 3.11.5.6-7 Unfactored Simplified Earth Pressure Distributions for Temporary Nongravity Cantilevered Walls with Continuous Vertical Wall Elements Embedded in Cohesive Soil and Retaining Cohesive Soil Modified After Teng (*1962*).

3.11.5.7 Apparent Earth Pressure (*AEP*) for Anchored Walls

For anchored walls constructed from the top down, the earth pressure may be estimated in accordance with Articles 3.11.5.7.1 or 3.11.5.7.2.

In developing the design pressure for an anchored wall, consideration shall be given to wall displacements that may affect adjacent structures and/or underground utilities.

3.11.5.7.1 Cohesionless Soils

The earth pressure on temporary or permanent anchored walls constructed in cohesionless soils may be determined using Figure 1, for which the maximum ordinate, p_a, of the pressure diagram is computed as follows:

C3.11.5.7

In the development of lateral earth pressures, the method and sequence of construction, the rigidity of the wall/anchor system, the physical characteristics and stability of the ground mass to be supported, allowable wall deflections, anchor spacing and prestress and the potential for anchor yield should be considered.

Several suitable apparent earth pressure distribution diagrams are available and in common use for the design of anchored walls, Sabatini et al. (*1999*); Cheney (*1988*); and U. S. Department of the Navy (*1982a*). Some of the apparent earth pressure diagrams, such as those described in Articles 3.11.5.7.1 and 3.11.5.7.2, are based on the results of measurements on anchored walls, Sabatini et al. (*1999*). Others are based on the results of measurements on strutted excavations, Terzaghi and Peck (*1967*), the results of analytical and scale model studies, Clough and Tsui (*1974*); Hanna and Matallana (*1970*), and observations of anchored wall installations (*Nicholson et al. 1981*); Schnabel (*1982*). While the results of these efforts provide somewhat different and occasionally conflicting results, they all tend to confirm the presence of higher lateral pressures near the top of the wall than would be predicted by classical earth pressure theories, due to the constraint provided by the upper level of anchors, and a generally uniform pressure distribution with depth.

For walls with one anchor level:

$$p_a = k_a \gamma'_s H \qquad (3.11.5.7.1\text{-}1)$$

For walls with multiple anchor levels:

$$p_a = \frac{k_a \gamma'_s H^2}{1.5H - 0.5H_1 - 0.5H_{n+1}} \qquad (3.11.5.7.1\text{-}2)$$

where:

p_a = maximum ordinate of pressure diagram (ksf)

k_a = active earth pressure coefficient
= $\tan^2 (45° - \phi_f/2)$ (dim.) for $\beta = 0$
use Eq. 3.11.5.3-1 for $\beta \neq 0$

γ'_s = effective unit weight of soil (kcf)

H = total excavation depth (ft.)

H_1 = distance from ground surface to uppermost ground anchor (ft.)

H_{n+1} = distance from base of excavation to lowermost ground anchor (ft.)

T_{hi} = horizontal load in ground anchor i (kip/ft.)

R = reaction force to be resisted by subgrade (i.e., below base of excavation) (kip/ft.)

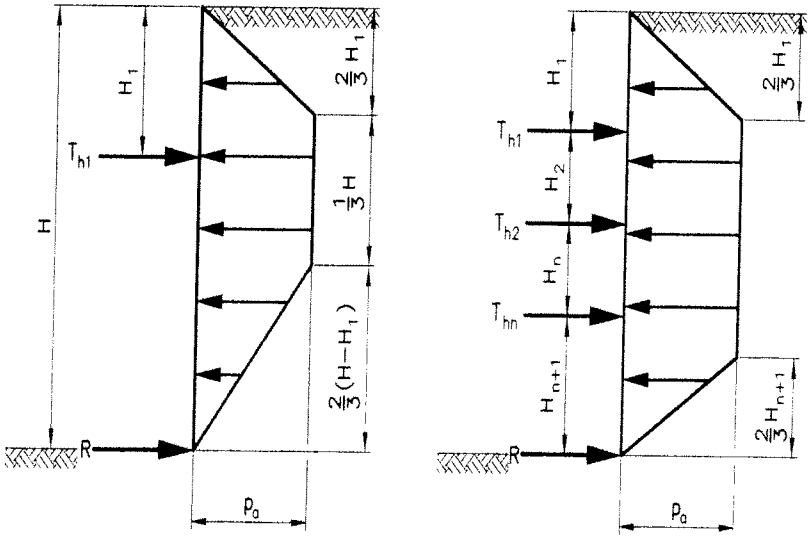

(a) Wall with one level of ground anchors

(b) Walls with multiple levels of ground anchors

Figure 3.11.5.7.1-1 Apparent Earth Pressure Distributions for Anchored Walls Constructed from the Top Down in Cohesionless Soils.

3.11.5.7.2 Cohesive Soils

The apparent earth pressure distribution for cohesive soils is related to the stability number, N_s, which is defined as:

$$N_s = \frac{\gamma_s H}{S_u} \qquad (3.11.5.7.2\text{-}1)$$

where:

γ_s = total unit weight of soil (kcf)

H = total excavation depth (ft.)

S_u = average undrained shear strength of soil (ksf)

3.11.5.7.2a Stiff to Hard

For temporary anchored walls in stiff to hard cohesive soils ($N_s \leq 4$), the earth pressure may be determined using Figure 3.11.5.7.1-1, with the maximum ordinate, p_a, of the pressure diagram computed as:

$$p_a = 0.2\gamma_s H \text{ to } 0.4\gamma_s H \qquad (3.11.5.7.2\text{a-}1)$$

where:

p_a = maximum ordinate of pressure diagram (ksf)

γ_s = total unit weight of soil (kcf)

H = total excavation depth (ft.)

For permanent anchored walls in stiff to hard cohesive soils, the apparent earth pressure distributions described in Article 3.11.5.7.1 may be used with k_a based on the drained friction angle of the cohesive soil. For permanent walls, the distribution, permanent or temporary, resulting in the maximum total force shall be used for design.

3.11.5.7.2b Soft to Medium Stiff

The earth pressure on temporary or permanent walls in soft to medium stiff cohesive soils ($N_s \geq 6$) may be determined using Figure 1, for which the maximum ordinate, p_a, of the pressure diagram is computed as:

$$p_a = k_a \gamma_s H \qquad (3.11.5.7.2\text{b-}1)$$

C3.11.5.7.2a

The determination of earth pressures in cohesive soils described in this Article and Article 3.11.5.7.2b are based on the results of measurements on anchored walls, Sabatini et al. (*1999*). In the absence of specific experience in a particular deposit, $p_a = 0.3\ \gamma_s\ H$ should be used for the maximum pressure ordinate when ground anchors are locked off at 75 percent of the unfactored design load or less. Where anchors are to be locked off at 100 percent of the unfactored design load or greater, a maximum pressure ordinate of $p_a = 0.4\ \gamma_s\ H$ should be used.

For temporary walls, the apparent earth pressure distribution in Figure 3.11.5.7.1-1 should only be used for excavations of controlled short duration, where the soil is not fissured and where there is no available free water.

Temporary loading may control design of permanent walls and should be evaluated in addition to permanent loading.

C3.11.5.7.2b

For soils with $4 < N_s < 6$, use the larger p_a from Eq. 3.11.5.7.2a-1 and Eq. 1.

where:

p_a = maximum ordinate of pressure diagram (ksf)

k_a = active earth pressure coefficient from Eq. 2

γ_s = total unit weight of soil (kcf)

H = total excavation depth (ft.)

The active earth pressure coefficient, k_a, may be determined by:

$$k_a = 1 - \frac{4S_u}{\gamma_s H} + 2\sqrt{2}\frac{d}{H}\left(\frac{1 - 5.14S_{ub}}{\gamma_s H}\right) \geq 0.22 \qquad (3.11.5.7.2b\text{-}2)$$

where:

S_u = undrained strength of retained soil (ksf)

S_{ub} = undrained strength of soil below excavation base (ksf)

γ_s = total unit weight of retained soil (kcf)

H = total excavation depth (ft.)

d = depth of potential base failure surface below base of excavation (ft.)

The value of d is taken as the thickness of soft to medium stiff cohesive soil below the excavation base up to a maximum value of $B_e/\sqrt{2}$, where B_e is the excavation width.

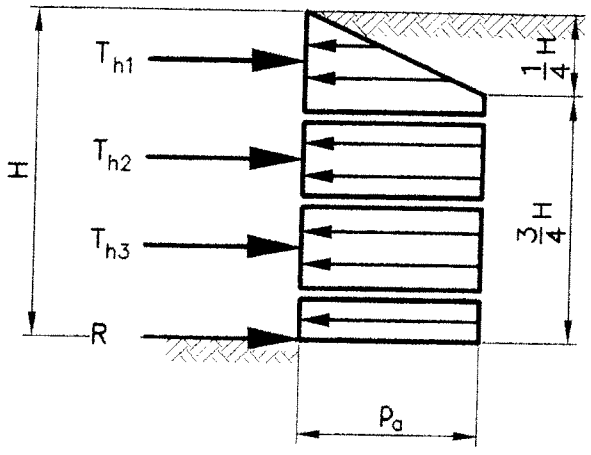

Figure 3.11.5.7.2b-1 Apparent Earth Pressure Distribution for Anchored Walls Constructed from the Top Down in Soft to Medium Stiff Cohesive Soils.

3.11.5.8 Lateral Earth Pressures for Mechanically Stabilized Earth Walls

3.11.5.8.1 General

The resultant force per unit width behind an MSE wall, shown in Figures 1, 2 and 3 as acting at a height of $h/3$ above the base of the wall, shall be taken as:

$$P_a = 0.5 k_a \gamma_s h^2 \qquad (3.11.5.8.1\text{-}1)$$

where:

P_a = force resultant per unit width (kip/ft.)

γ_s = total unit weight of backfill (kcf)

h = height of horizontal earth pressure diagram taken as shown in Figures 1, 2 and 3 (ft.)

k_a = active earth pressure coefficient specified in Article 3.11.5.3, with the angle of backfill slope taken as β, as specified in Figure 2, B, as specified in Figure 3, and $\delta=\beta$ and B in Figures 2 and 3, respectively.

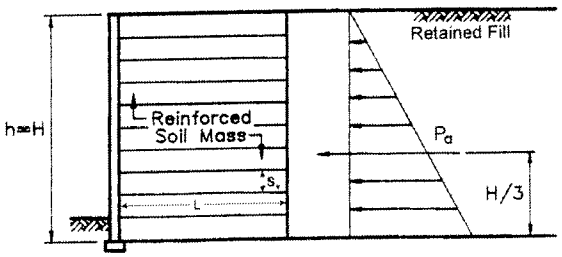

Figure 3.11.5.8.1-1 Earth Pressure Distribution for MSE Wall with Level Backfill Surface.

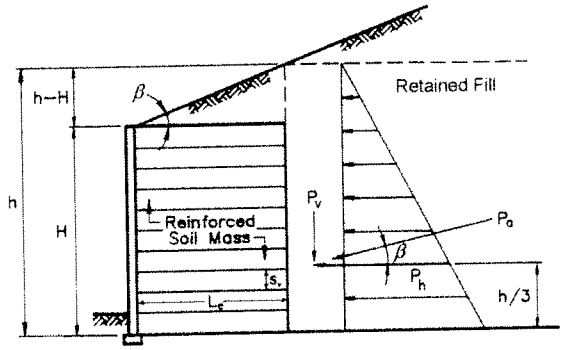

Figure 3.11.5.8.1-2 Earth Pressure for MSE Wall with Sloping Backfill Surface.

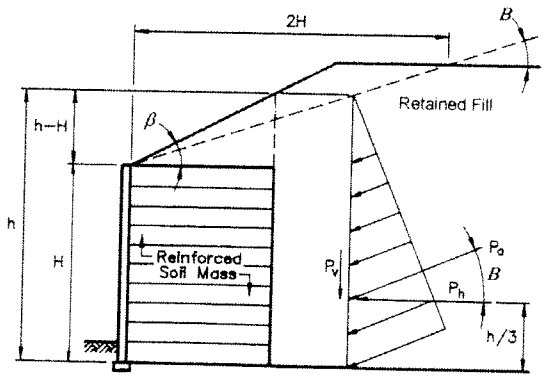

Figure 3.11.5.8.1-3 Earth Pressure Distribution for MSE Wall with Broken Back Backfill Surface.

3.11.5.8.2 Internal Stability

The load factor γ_p to be applied to the maximum load carried by the reinforcement T_{max} for reinforcement strength, connection strength, and pullout calculations (see Article 11.10.6.2) shall be *EV*, for vertical earth pressure.

For MSE walls η_i shall be taken as 1.

C3.11.5.8.2

Loads carried by the soil reinforcement in mechanically stabilized earth walls are the result of vertical and lateral earth pressures which exist within the reinforced soil mass, reinforcement extensibility, facing stiffness, wall toe restraint, and the stiffness and strength of the soil backfill within the reinforced soil mass. The calculation method for T_{max} is empirically derived, based on reinforcement strain measurements, converted to load based on the reinforcement modulus, from full scale walls at working stress conditions. The load factor *EV*, on the other hand, was determined in consideration of vertical earth pressure exerted by a soil mass without inclusions, and was calibrated to address uncertainties implied by allowable stress design for external stability for walls. *EV* is not directly applicable to internal reinforcement loads in MSE walls, since the calibration of *EV* was not performed with internal stability of a reinforced system in mind.

The use of *EV* for the load factor in this case should be considered an interim measure until research is completed to quantify load prediction bias and uncertainty.

3.11.5.9 Lateral Earth Pressures for Prefabricated Modular Walls

The magnitude and location of resultant loads and resisting forces for prefabricated modular walls may be determined using the earth pressure distributions presented in Figures 1 and 2. Where the back of the prefabricated modules forms an irregular, stepped surface, the earth pressure shall be computed on a plane surface drawn from the upper back corner of the top module to the lower back heel of the bottom module using Coulomb earth pressure theory.

C3.11.5.9

Prefabricated modular walls are gravity walls constructed of prefabricated concrete elements that are in-filled with soil. They differ from modular block MSE structures in that they contain no soil reinforcing elements.

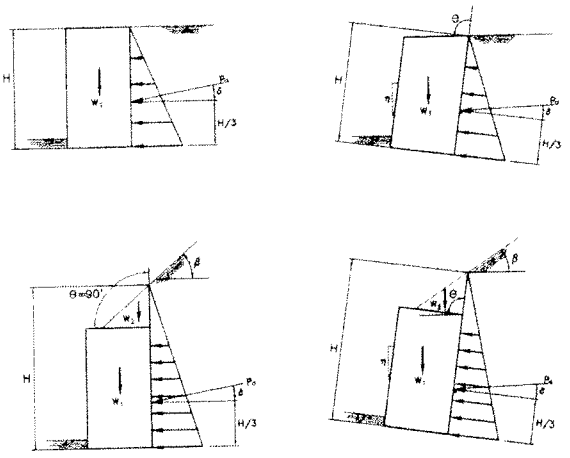

$$P_a @ \frac{H}{3}$$

$$P_a = \frac{1}{2}\gamma_s' H^2 k_a$$

Figure 3.11.5.9-1 Earth Pressure Distributions for Prefabricated Modular Walls with Continuous Pressure Surfaces.

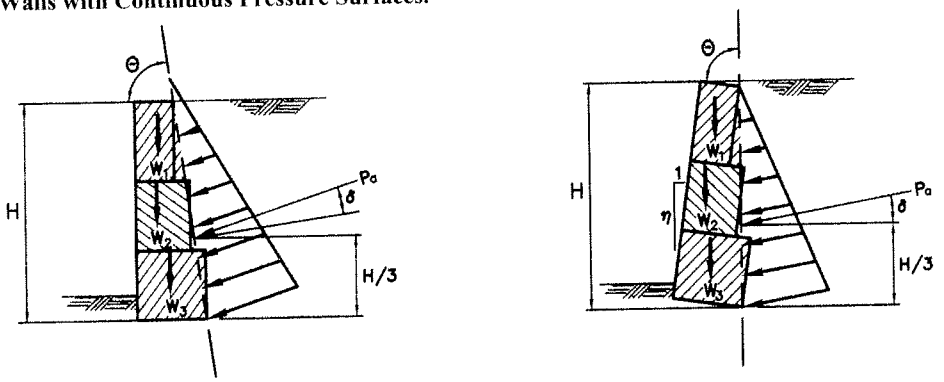

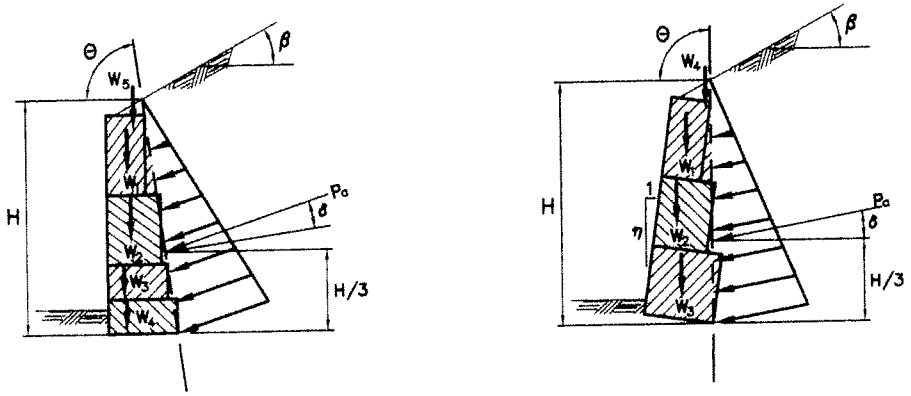

Figure 3.11.5.9-2 Earth Pressure Distributions for Prefabricated Modular Walls with Irregular Pressure Surfaces.

The value of k_a used to compute lateral thrust resulting from retained backfill and other loads behind the wall shall be computed based on the friction angle of the backfill behind the modules. In the absence of specific data, if granular backfill is used behind the prefabricated modules within a zone of at least $1V$:$1H$ from the heal of the wall, a value of 34° may be used for ϕ_f. Otherwise, without specific data, a maximum friction angle of 30° shall be used.

The wall friction angle, δ, is a function of the direction and magnitude of possible movements, and the properties of the backfill. When the structure settles more than the backfill, the wall friction angle is negative.

As a maximum, the wall friction angles, given in Table C1, should be used to compute k_a, unless more exact coefficients are demonstrated:

Table C3.11.5.9-1 Maximum Wall Friction Angles, δ.

Case	Wall Friction Angle (δ)
Modules settle more than backfill	0
Continuous pressure surface of precast concrete (uniform width modules)	0.50 ϕ_f
Average pressure surface (stepped modules)	0.75 ϕ_f

3.11.6 Surcharge Loads: *ES* and *LS*

The factored soil stress increase behind or within the wall caused by concentrated surcharge loads or stresses shall be the greater of (1) the unfactored surcharge loads or stresses multiplied by the specified load factor, *ES*, or (2) the factored loads for the structure as applied to the structural element causing the surcharge load, setting *ES* to 1.0. The load applied to the wall due to the structural element above the wall shall not be double factored.

Concentrated surcharge loads induced by foundations are typically the result of dead load, live load, wind load, and possibly other loads that are associated with load factors other than *ES*. However, the controlling uncertainty in load prediction for surcharges is the transmission of the surcharge load through the soil to the wall or other structure below the surcharge. Hence, *ES* should be applied to the unfactored concentrated surcharge loads, unless the combined effect of the factored loads applicable to the foundation unit transmitting load to the top of the wall is more conservative. In this latter case, *ES* should be set equal to 1.0 and the factored footing loads used as the concentrated surcharge load in the wall design.

3.11.6.1 Uniform Surcharge Loads (*ES*)

Where a uniform surcharge is present, a constant horizontal earth pressure shall be added to the basic earth pressure. This constant earth pressure may be taken as:

$$\Delta_p = k_s q_s \qquad (3.11.6.1\text{-}1)$$

where:

Δ_p = constant horizontal earth pressure due to uniform surcharge (ksf)

k_s = coefficient of earth pressure due to surcharge

q_s = uniform surcharge applied to the upper surface of the active earth wedge (ksf)

C3.11.6.1

When the uniform surcharge is produced by an earth loading on the upper surface, the load factor for both vertical and horizontal components shall be taken as specified in Table 3.4.1-2 for earth surcharge.

For active earth pressure conditions, k_s shall be taken as k_a, and for at-rest conditions, k_s shall be taken as k_o. Otherwise, intermediate values appropriate for the type of backfill and amount of wall movement may be used.

3.11.6.2 Point, Line and Strip Loads (*ES*)—Walls Restrained from Movement

The horizontal pressure, Δ_{ph} in ksf, on a wall resulting from a uniformly loaded strip parallel to the wall may be taken as:

$$\Delta_{ph} = \frac{2p}{\pi}[\delta - \sin\delta\cos(\delta + 2\alpha)] \qquad (3.11.6.2\text{-}1)$$

where:

p = uniform load intensity on strip parallel to wall (ksf)

α = angle specified in Figure 1 (rad.)

δ = angle specified in Figure 1 (rad.)

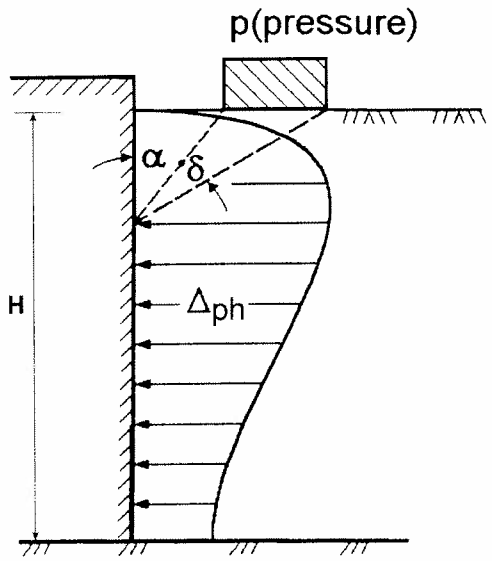

Figure 3.11.6.2-1 Horizontal Pressure on Wall Caused by a Uniformly Loaded Strip.

The horizontal pressure, Δ_{ph} in ksf, on a wall resulting from a point load may be taken as:

$$\Delta_{ph} = \frac{P}{\pi R^2}\left[\frac{3ZX^2}{R^3} - \frac{R(1-2\nu)}{R+Z}\right] \qquad (3.11.6.2\text{-}2)$$

where:

P = point load (kip)

Wall movement needed to mobilize extreme active and passive pressures for various types of backfill can be found in Table C3.11.1-1.

C3.11.6.2

Eqs. 2, 3, 4, and 5 are based on the assumption that the wall does not move, i.e., walls which have a high degree of structural rigidity or restrained at the top combined with an inability to slide in response to applied loads. For flexible walls, this assumption can be very conservative. Additional guidance regarding the ability of walls to move is provided in Articles C3.11.1 and A11.1.1.3.

R = radial distance from point of load application to a point on the wall as specified in Figure 2 where $R = (x^2 + y^2 + z^2)^{0.5}$ (ft.)

X = horizontal distance from back of wall to point of load application (ft.)

Y = horizontal distance from point on the wall under consideration to a plane, which is perpendicular to the wall and passes through the point of load application measured along the wall (ft.)

Z = vertical distance from point of load application to the elevation of a point on the wall under consideration (ft.)

ν = Poisson's ratio (dim.)

The point on the wall does not have to lie in a plane which is perpendicular to the wall and passes through the point of load application.

Poisson's ratio for soils varies from about 0.25 to 0.49, with lower values more typical for granular and stiff cohesive soils and higher values more typical for soft cohesive soils.

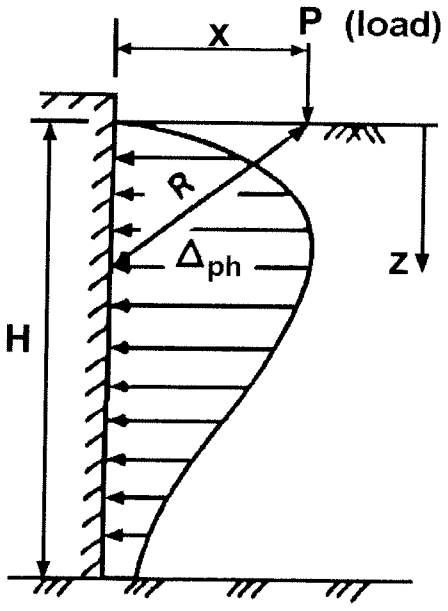

Figure 3.11.6.2-2 Horizontal Pressure on a Wall Caused by a Point Load.

The horizontal pressure, Δ_{ph} in ksf, resulting from an infinitely long line load parallel to a wall may be taken as:

$$\Delta_{ph} = \frac{4Q}{\pi} \frac{X^2 Z}{R^4} \qquad (3.11.6.2\text{-}3)$$

where:

Q = load intensity in kip/ft.

and all other notation is as defined above and shown in Figure 3.

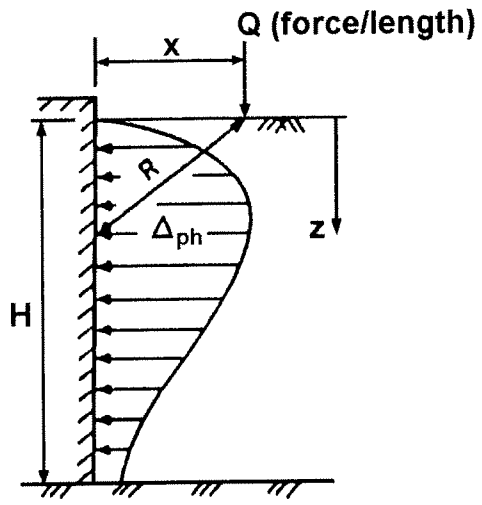

Figure 3.11.6.2-3 Horizontal Pressure on a Wall Caused by an Infinitely Long Line Load Parallel to the Wall.

The horizontal pressure distribution, Δ_{ph} in ksf, on a wall resulting from a finite line load perpendicular to a wall may be taken as:

$$\Delta_{ph} = \frac{Q}{\pi Z}\left(\frac{1}{A^3} - \frac{1-2\nu}{A+\frac{Z}{X_2}} - \frac{1}{B^3} + \frac{1-2\nu}{B+\frac{Z}{X_1}}\right) \tag{3.11.6.2-4}$$

in which:

$$A = \sqrt{1+\left(\frac{Z}{X_2}\right)^2} \tag{3.11.6.2-5}$$

$$B = \sqrt{1+\left(\frac{Z}{X_1}\right)^2} \tag{3.11.6.2-6}$$

where:

X_1 = distance from the back of the wall to the start of the line load as specified in Figure 4 (ft.)

X_2 = length of the line load (ft.)

Z = depth from the ground surface to a point on the wall under consideration (ft.)

ν = Poisson's Ratio (dim.)

Q = load intensity (kip/ft.)

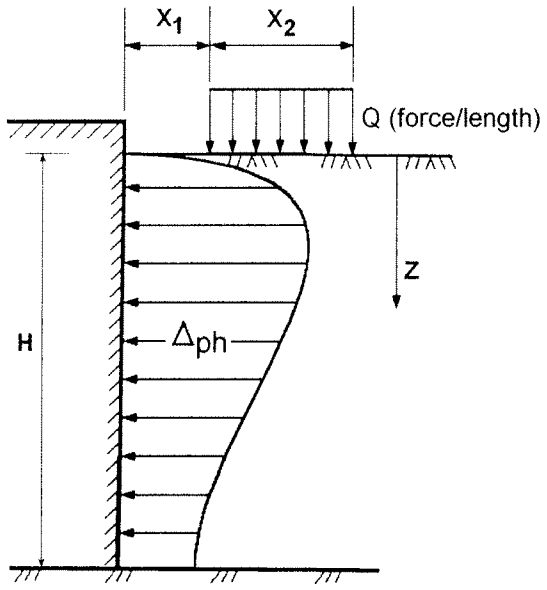

Figure 3.11.6.2-4 Horizontal Pressure on a Wall Caused by a Finite Line Load Perpendicular to the Wall.

3.11.6.3 Strip Loads (*ES*)—Flexible Walls

Concentrated dead loads shall be incorporated into the internal and external stability design by using a simplified uniform vertical distribution of 2 vertical to 1 horizontal to determine the vertical component of stress with depth within the reinforced soil mass as specified in Figure 1. Concentrated horizontal loads at the top of the wall shall be distributed within the reinforced soil mass as specified in Figure 2. If concentrated dead loads are located behind the reinforced soil mass, they shall be distributed in the same way as would be done within the reinforced soil mass.

The vertical stress distributed behind the reinforced zone shall be multiplied by k_a when determining the effect of this surcharge load on external stability. The concentrated horizontal stress distributed behind the wall as specified in Figure 2 shall not be multiplied by k_a.

C3.11.6.3

Figures 1 and 2 are based on the assumption that the wall is relatively free to move laterally (e.g., MSE walls).

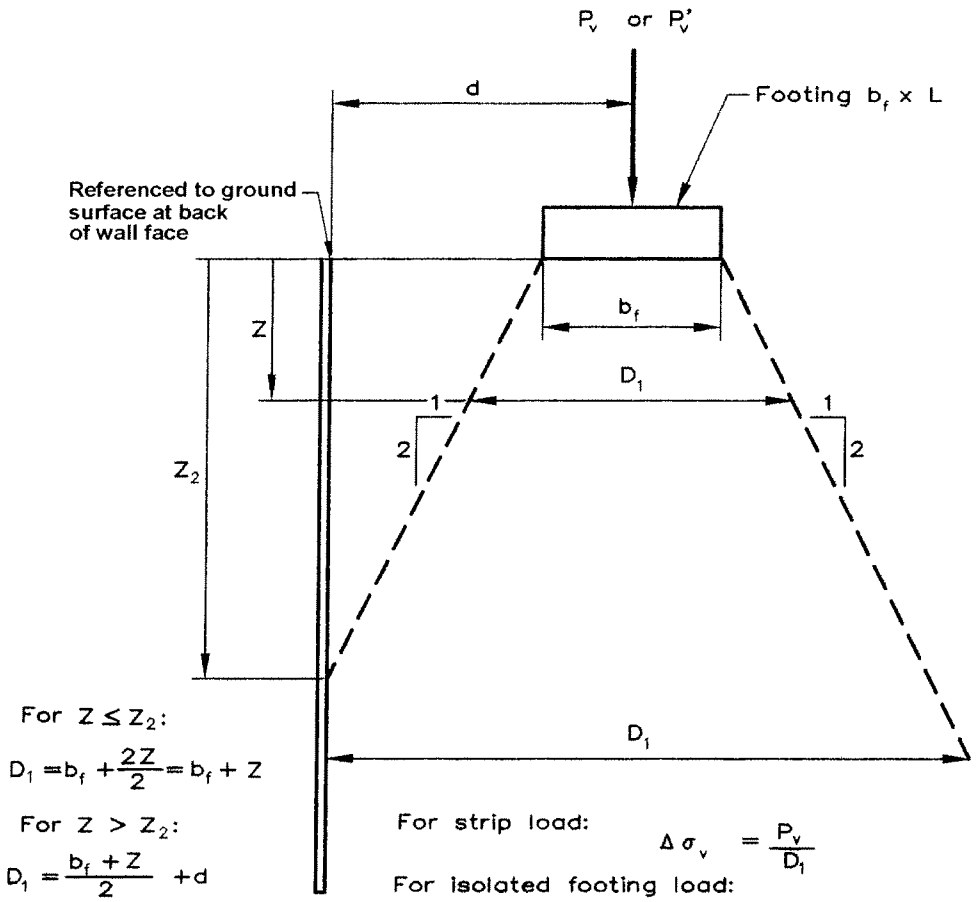

Where: D_1 = Effective width of applied load at any depth, calculated as shown above

b_f = Width of applied load. For footings which are eccentrically loaded (e.g., bridge abutment footings), set b_f equal to the equivalent footing width B' by reducing it by 2e', where e' is the eccentricity of the footing load (i.e., $b_f - 2e'$).

L = Length of footing

P_v = Load per linear foot of strip footing

P_v' = Load on isolated rectangular footing or point load

Z_2 = depth where effective width intersects back of wall face = $2d - b_f$

d = distance between the centroid of the concentrated vertical load and the back of the wall face.

Assume the increased vertical stress due to the surcharge load has no influence on stresses used to evaluate internal stability if the surcharge load is located behind the reinforced soil mass. For external stability, assume the surcharge has no influence if it is located outside the active zone behind the wall.

Figure 3.11.6.3-1 Distribution of Stress from Concentrated Vertical Load P_v for Internal and External Stability Calculations.

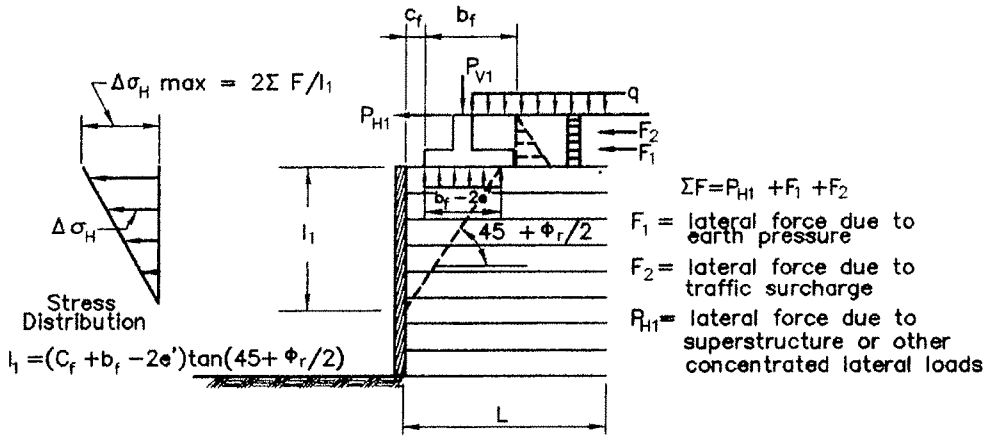

e' = eccentricity of load on footing (see Figure 11.10.10.1-1 for example of how to calculate this)

a. Distribution of Stress for Internal Stability Calculations.

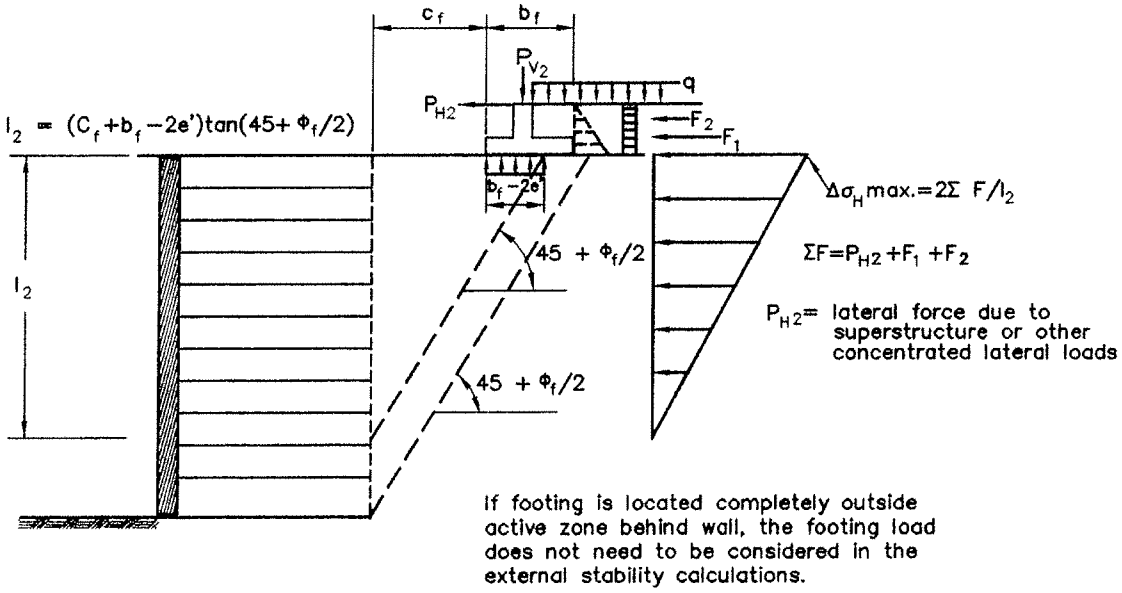

b. Distribution of Stress for External Stability Calculations.

Figure 3.11.6.3-2 Distribution of Stress from Concentrated Horizontal Loads.

3.11.6.4 Live Load Surcharge (*LS*)

A live load surcharge shall be applied where vehicular load is expected to act on the surface of the backfill within a distance equal to one-half the wall height behind the back face of the wall. If the surcharge is for a highway, the intensity of the load shall be consistent with the provisions of Article 3.6.1.2. If the surcharge is for other than a highway, the Owner shall specify and/or approve appropriate surcharge loads.

The increase in horizontal pressure due to live load surcharge may be estimated as:

C3.11.6.4

The tabulated values for h_{eq} were determined by evaluating the horizontal force against an abutment or wall from the pressure distribution produced by the vehicular live load of Article 3.6.1.2. The pressure distributions were developed from elastic half-space solutions using the following assumptions:

- Vehicle loads are distributed through a two-layer system consisting of pavement and soil subgrade

$$\Delta_p = k\gamma_s h_{eq} \qquad (3.11.6.4\text{-}1)$$

where:

Δ_p = constant horizontal earth pressure due to live load surcharge (ksf)

γ_s = total unit weight of soil (kcf)

k = coefficient of lateral earth pressure

h_{eq} = equivalent height of soil for vehicular load (ft.)

Equivalent heights of soil, h_{eq}, for highway loadings on abutments and retaining walls may be taken from Tables 1 and 2. Linear interpolation shall be used for intermediate wall heights.

The wall height shall be taken as the distance between the surface of the backfill and the bottom of the footing along the pressure surface being considered.

Table 3.11.6.4-1 Equivalent Height of Soil for Vehicular Loading on Abutments Perpendicular to Traffic.

Abutment Height (ft.)	h_{eq} (ft.)
5.0	4.0
10.0	3.0
≥20.0	2.0

Table 3.11.6.4-2 Equivalent Height of Soil for Vehicular Loading on Retaining Walls Parallel to Traffic.

Retaining Wall Height (ft.)	h_{eq} (ft.) Distance from wall backface to edge of traffic	
	0.0 ft.	1.0 ft. or Further
5.0	5.0	2.0
10.0	3.5	2.0
≥20.0	2.0	2.0

The load factor for both vertical and horizontal components of live load surcharge shall be taken as specified in Table 3.4.1-1 for live load surcharge.

3.11.6.5 Reduction of Surcharge

If the vehicular loading is transmitted through a structural slab, which is also supported by means other than earth, a corresponding reduction in the surcharge loads may be permitted.

- Poisson's ratio for the pavement and subgrade materials are 0.2 and 0.4, respectively
- Wheel loads were modeled as a finite number of point loads distributed across the tire area to produce an equivalent tire contact stress
- The process for equating wall moments resulting from the elastic solution with the equivalent surcharge method used a wall height increment of 0.25 ft.

The value of the coefficient of lateral earth pressure k is taken as k_o, specified in Article 3.11.5.2, for walls that do not deflect or move, or k_a, specified in Articles 3.11.5.3, 3.11.5.6 and 3.11.5.7, for walls that deflect or move sufficiently to reach minimum active conditions.

The analyses used to develop Tables 1 and 2 are presented in Kim and Barker (*1998*).

The values for h_{eq} given in Tables 1 and 2 are generally greater than the traditional 2.0 ft. of earth load historically used in the AASHTO specifications, but less than those prescribed in previous editions (i.e., before 1998) of this specification. The traditional value corresponds to a 20.0-kip single unit truck formerly known as an H10 truck, Peck et al. (*1974*). This partially explains the increase in h_{eq} in previous editions of this specification. Subsequent analyses, i.e., Kim and Barker (*1998*) show the importance of the direction of traffic, i.e., parallel for a wall and perpendicular for an abutment on the magnitude of h_{eq}. The magnitude of h_{eq} is greater for an abutment than for a wall due to the proximity and closer spacing of wheel loads to the back of an abutment compared to a wall.

The backface of the wall should be taken as the pressure surface being considered. Refer to Article C11.5.5 for application of surcharge pressures on retaining walls.

C3.11.6.5

This Article relates primarily to approach slabs which are supported at one edge by the backwall of an abutment, thus transmitting load directly thereto.

3.11.7 Reduction Due to Earth Pressure

For culverts and bridges and their components where earth pressure may reduce effects caused by other loads and forces, such reduction shall be limited to the extent earth pressure can be expected to be permanently present. In lieu of more precise information, a 50 percent reduction may be used, but need not be combined with the minimum load factor specified in Table 3.4.1-2.

3.11.8 Downdrag

Possible development of downdrag on piles or shafts shall be evaluated where:

- Sites are underlain by compressible material such as clays, silts or organic soils,
- Fill will be or has recently been placed adjacent to the piles or shafts, such as is frequently the case for bridge approach fills,
- The groundwater is substantially lowered, or
- Liquefaction of loose sandy soil can occur.

When the potential exists for downdrag to act on a pile or shaft due to downward movement of the soil relative to the pile or shaft, and the potential for downdrag is not eliminated by preloading the soil to reduce downward movements or other mitigating measure, the pile or shaft shall be designed to resist the induced downdrag.

Consideration shall be given to eliminating the potential for downdrag loads through the use of embankment surcharge loads, ground improvement techniques, and/or vertical drainage and settlement monitoring measurements.

For Extreme Event I limit state, downdrag induced by liquefaction settlement shall be applied to the pile or shaft in combination with the other loads included within that load group. Liquefaction-induced downdrag shall not be combined with downdrag induced by consolidation settlements.

For downdrag load applied to pile or shaft groups, group effects shall be evaluated.

C3.11.7

This provision is intended to refine the traditional approach in which the earth pressure is reduced by 50 percent in order to obtain maximum positive moment in top slab of culverts and frames. It permits obtaining more precise estimates of force effects where earth pressures are present.

C3.11.8

Downdrag, also known as negative skin friction, can be caused by soil settlement due to loads applied after the piles were driven, such as an approach embankment as shown in Figure C1. Consolidation can also occur due to recent lowering of the groundwater level as shown in Figure C2.

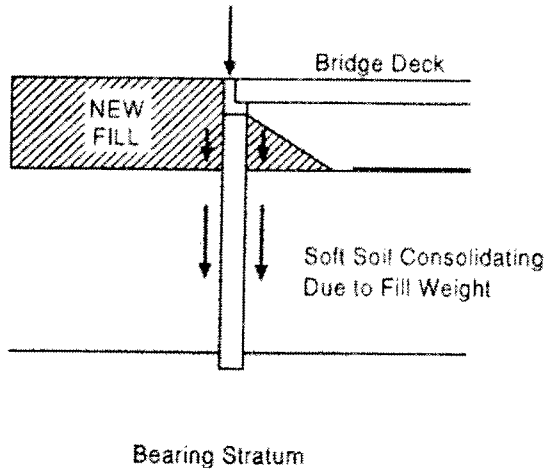

Figure C3.11.8-1 Common Downdrag Situation Due to Fill Weight (Hannigan, et al. *2005*).

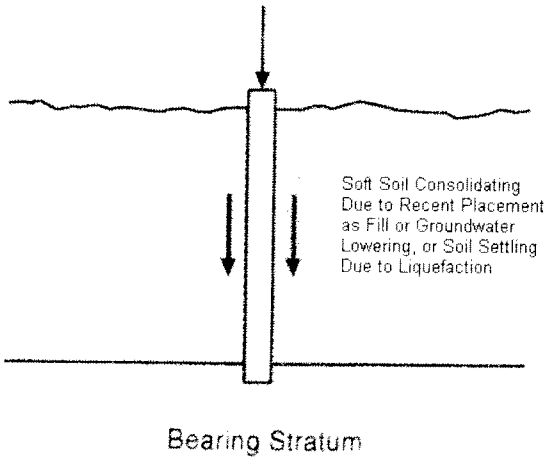

Figure C3.11.8-2 Common Downdrag Situation Due to Causes Other than Recent Fill Placement.

Regarding the load factors for downdrag in Table 3.4.1-2, use the maximum load factor when investigating maximum downward pile loads. The minimum load factor shall only be utilized when investigating possible uplift loads.

For some downdrag estimation methods, the magnitude of the load factor is dependent on the magnitude of the downdrag load relative to the dead load. The downdrag load factors were developed considering that downdrag loads equal to or greater than the magnitude of the dead load become somewhat impractical for design. See Allen (*2005*) for additional background and guidance on the effect of downdrag load magnitude.

Methods for eliminating static downdrag potential include preloading. The procedure for designing a preload is presented in Cheney and Chassie (*2000*).

Post-liquefaction settlement can also cause downdrag. Methods for mitigating liquefaction-induced downdrag are presented in Kavazanjian, et al. (*1997*).

The application of downdrag to pile or shaft groups can be complex. If the pile or shaft cap is near or below the fill material causing consolidation settlement of the underlying soft soil, the cap will prevent transfer of stresses adequate to produce settlement of the soil inside the pile or shaft group. The downdrag applied in this case is the frictional force around the exterior of the pile or shaft group and along the sides of the pile or shaft cap (if any). If the cap is located well up in the fill causing consolidation stresses or if the piles or shafts are used as individual columns to support the structure above ground, the downdrag on each individual pile or shaft will control the magnitude of the load. If group effects are likely, the downdrag calculated using the group perimeter shear force should be determined in addition to the sum of the downdrag forces for each individual pile or shaft. The greater of the two calculations should be used for design.

The skin friction used to estimate downdrag due to liquefaction settlement should be conservatively assumed to be equal to the residual soil strength in the liquefiable zone, and nonliquefied skin friction in nonliquefiable layers above the zone of liquefaction.

Transient loads can act to reduce the downdrag because they cause a downward movement of the pile resulting in a temporary reduction or elimination of the downdrag load. It is conservative to include the transient loads together with downdrag.

The step-by-step procedure for determining downdrag is presented in detail in Hannigan, et al. (*2005*).

If transient loads act to reduce the magnitude of downdrag loads and this reduction is considered in the design of the pile or shaft, the reduction shall not exceed that portion of transient load equal to the downdrag force effect.

Force effects due to downdrag on piles or drilled shafts should be determined as follows:

Step 1—Establish soil profile and soil properties for computing settlement using the procedures in Article 10.4.

Step 2—Perform settlement computations for the soil layers along the length of the pile or shaft using the procedures in Article 10.6.2.4.3.

Step 3—Determine the length of pile or shaft that will be subject to downdrag. If the settlement in the soil layer is 0.4 in. or greater relative to the pile or shaft, downdrag can be assumed to fully develop.

The stress increases in each soil layer due to embankment load can be estimated using the procedures in Hannigan et al. (*2005*) or Cheney and Chassie (*2000*).

If the settlement is due to liquefaction, the Tokimatsu and Seed (*1987*) or the Ishihara and Yoshimine (*1992*) procedures can be used to estimate settlement.

Step 4—Determine the magnitude of the downdrag, *DD*, by computing the negative skin resistance using any of the static analysis procedures in Article 10.7.3.8.6 for piles in all soils and Article 10.8.3.4 for shafts if the zone subject to downdrag is characterized as a cohesive soil. If the downdrag zone is characterized as a cohesionless soil, the procedures provided in Article 10.8.3.4 should be used to estimate the downdrag for shafts. Sum the negative skin resistance for all layers contributing to downdrag from the lowest layer to the bottom of the pile cap or ground surface.

The neutral plane method may also be used to determine downdrag.

The methods used to estimate downdrag are the same as those used to estimate skin friction, as described in Articles 10.7 and 10.8. The distinction between the two is that downdrag acts downward on the sides of the piles or shafts and loads the foundation, whereas skin friction acts upward on the sides of piles or shafts and, thus, supports the foundation loads.

Downdrag can be estimated for piles using the α or λ methods for cohesive soils. An alternative approach would be to use the β method where the long-term conditions after consolidation should be considered. Cohesionless soil layers overlying the consolidating layers will also contribute to downdrag, and the negative skin resistance in these layers should be estimated using an effective stress method.

Downdrag loads for shafts may be estimated using the α method for cohesive soils and the β method for granular soils, as specified in Article 10.8, for calculating negative shaft resistance. As with positive shaft resistance, the top 5.0 ft. and a bottom length taken as one shaft diameter do not contribute to downdrag loads. When using the α method, an allowance should be made for a possible increase in the undrained shear strength as consolidation occurs.

The neutral plane method is described and discussed in NCHRP 393 (Briaud and Tucker, *1993*).

3.12 FORCE EFFECTS DUE TO SUPERIMPOSED DEFORMATIONS: *TU, TG, SH, CR, SE*

3.12.1 General

Internal force effects in a component due to creep and shrinkage shall be considered. The effect of a temperature gradient should be included where appropriate. Force effects resulting from resisting component deformation, displacement of points of load application, and support movements shall be included in the analysis.

3.12.2 Uniform Temperature

The design thermal movement associated with a uniform temperature change may be calculated using Procedure A or Procedure B below. Either Procedure A or Procedure B may be employed for concrete deck bridges having concrete or steel girders. Procedure A shall be employed for all other bridge types.

3.12.2.1 Temperature Range for Procedure A

The ranges of temperature shall be as specified in Table 1. The difference between the extended lower or upper boundary and the base construction temperature assumed in the design shall be used to calculate thermal deformation effects.

C3.12.2.1

Procedure A is the historic method that has been used for bridge design.

For these Specifications, a moderate climate may be determined by the number of freezing days per year. If the number of freezing days is less than 14, the climate is considered to be moderate. Freezing days are days when the average temperature is less than 32°F.

The minimum and maximum temperatures specified in Table 1 shall be taken as $T_{MinDesign}$ and $T_{MaxDesign}$, respectively, in Eq. 3.12.2.3-1.

Although temperature changes in a bridge do not occur uniformly, bridges generally are designed for an assumed uniform temperature change. The orientation of bearing guides and the freedom of bearing movement is important. Sharp curvature and sharply skewed supports can cause excessive lateral thermal forces at supports if only tangential movement is permitted. Wide bridges are particularly prone to large lateral thermal forces because the bridge expands radially as well as longitudinally.

Table 3.12.2.1-1 Procedure A Temperature Ranges.

CLIMATE	STEEL OR ALUMINUM	CONCRETE	WOOD
Moderate	0° to 120°F	10° to 80°F	10° to 75°F
Cold	−30° to 120°F	0° to 80°F	0° to 75°F

3.12.2.2 Temperature Range for Procedure B

The temperature range shall be defined as the difference between the maximum design temperature, $T_{MaxDesign}$, and the minimum design temperature, $T_{MinDesign}$. For all concrete girder bridges with concrete decks, $T_{MaxDesign}$ shall be determined from the contours of Figure 1 and $T_{MinDesign}$ shall be determined from the contours of Figure 2. For steel girder bridges with concrete decks, $T_{MaxDesign}$ shall be determined from the contours of Figure 3 and $T_{MinDesign}$ shall be determined from the contours of Figure 4.

C3.12.2.2

The Procedure B design was developed on the basis of the report "Thermal Movement Design Procedure for Steel and Concrete Bridges" *(Roeder 2002)*.

Procedure B is a calibrated procedure and does not cover all bridge types. The temperatures provided in the maps of Figures 1 to 4 are extreme bridge design temperatures for an average history of 70 years with a minimum of 60 years of data for locations throughout the U.S.

The design values for locations between contours should be determined by linear interpolation. As an alternative method, the largest adjacent contour may be used to define $T_{MaxDesign}$ and the smallest adjacent contour may be used to define $T_{MinDesign}$. Both the minimum and maximum design temperatures should be noted on the drawings for the girders, expansion joints, and bearings.

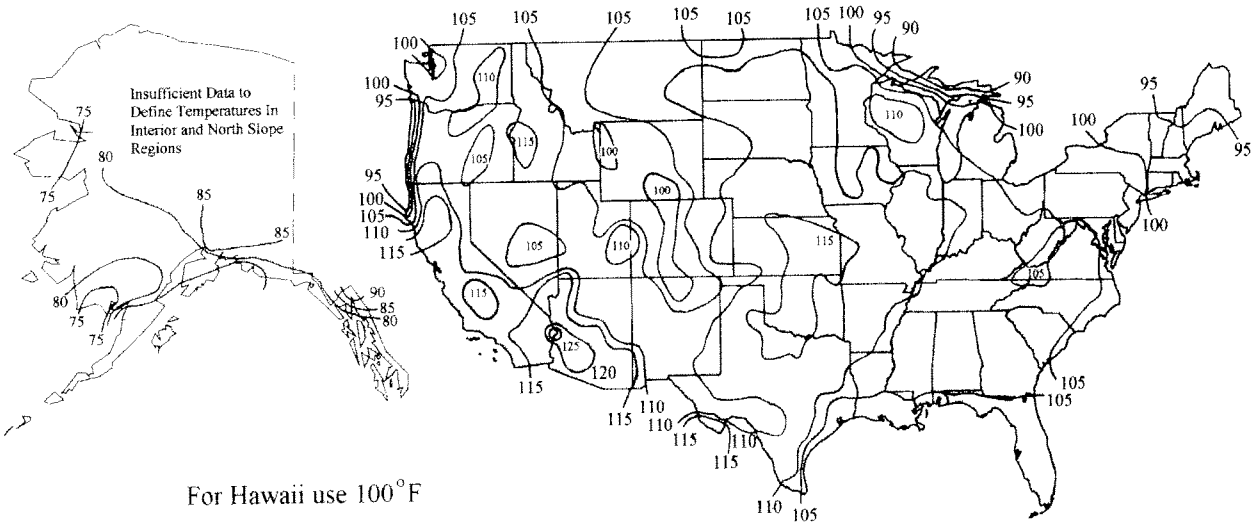

Figure 3.12.2.2-1 Contour Maps for $T_{MaxDesign}$ for Concrete Girder Bridges with Concrete Decks.

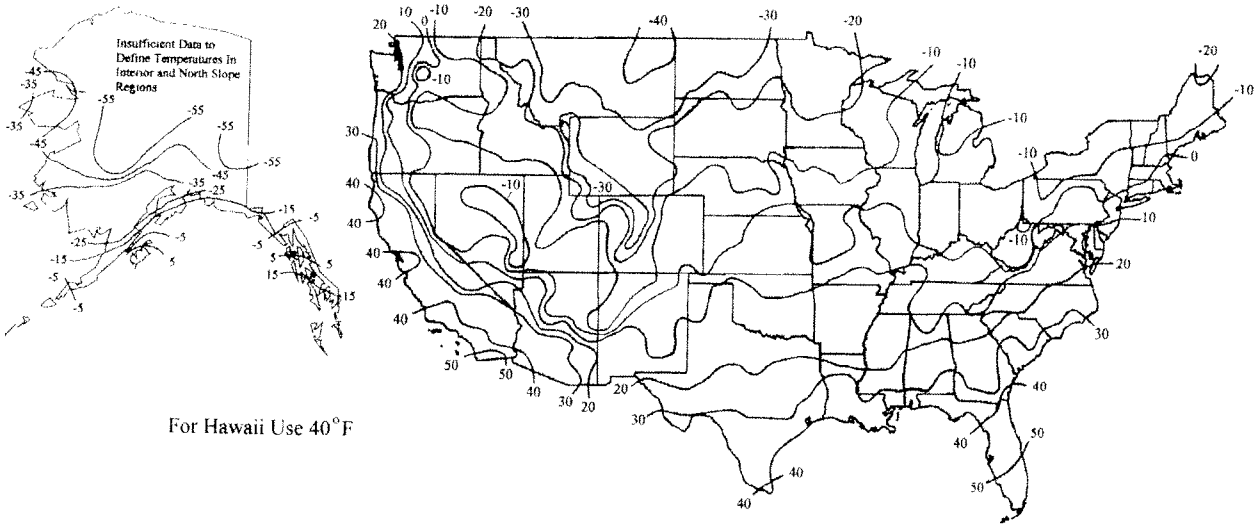

Figure 3.12.2.2-2 Contour Maps for $T_{MinDesign}$ for Concrete Girder Bridges with Concrete Decks.

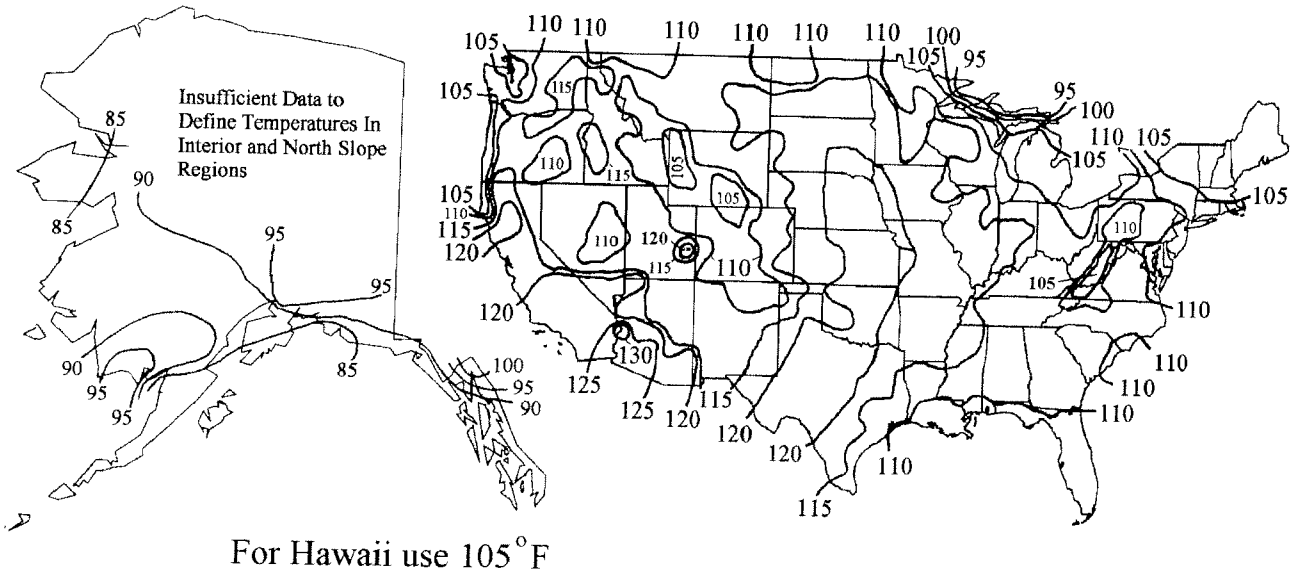

Figure 3.12.2.2-3 Contour Maps for $T_{MaxDesign}$ for Steel Girder Bridges with Concrete Decks.

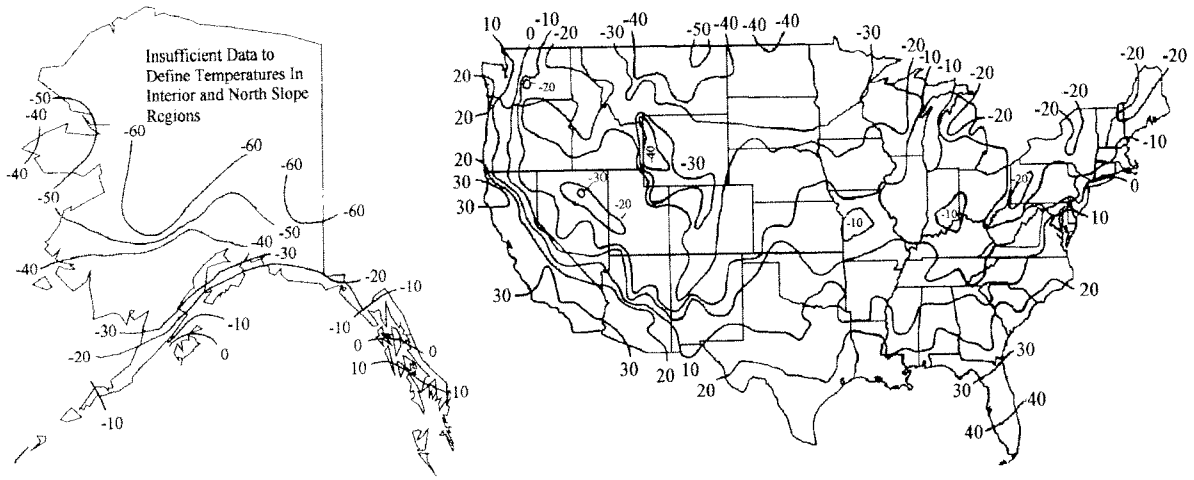

Figure 3.12.2.2-4 Contour Maps for $T_{MinDesign}$ for Steel Girder Bridges with Concrete Decks.

3.12.2.3 Design Thermal Movements

The design thermal movement range, Δ_T, shall depend upon the extreme bridge design temperatures defined in Article 3.12.2.1 or 3.12.2.2, and be determined as:

$$\Delta_T = \alpha L (T_{MaxDesign} - T_{MinDesign}) \qquad (3.12.2.3\text{-}1)$$

where:

L = expansion length (in.)

α = coefficient of thermal expansion (in./in./°F)

3.12.3 Temperature Gradient

For the purpose of this Article, the country shall be subdivided into zones as indicated in Figure 1. Positive temperature values for the zones shall be taken as specified for various deck surface conditions in Table 1. Negative temperature values shall be obtained by multiplying the values specified in Table 1 by −0.30 for plain concrete decks and −0.20 for decks with an asphalt overlay.

The vertical temperature gradient in concrete and steel superstructures with concrete decks may be taken as shown in Figure 2.

Dimension A in Figure 2 shall be taken as:

C3.12.3

Temperature gradient is included in various load combinations in Table 3.4.1-1. This does not mean that it need be investigated for all types of structures. If experience has shown that neglecting temperature gradient in the design of a given type of structure has not lead to structural distress, the Owner may choose to exclude temperature gradient. Multibeam bridges are an example of a type of structure for which judgment and past experience should be considered.

Redistribution of reactive loads, both longitudinally and transversely, should also be calculated and considered in the design of the bearings and substructures.

- For concrete superstructures that are 16.0 in. or more in depth—12.0 in.
- For concrete sections shallower than 16.0 in.—4.0 in. less than the actual depth
- For steel superstructures—12.0 in. and the distance t shall be taken as the depth of the concrete deck

Temperature value T_3 shall be taken as 0.0°F, unless a site-specific study is made to determine an appropriate value, but it shall not exceed 5°F.

Where temperature gradient is considered, internal stresses and structure deformations due to both positive and negative temperature gradients may be determined in accordance with the provisions of Article 4.6.6.

Table 3.12.3-1 Basis for Temperature Gradients.

Zone	T_1 (°F)	T_2 (°F)
1	54	14
2	46	12
3	41	11
4	38	9

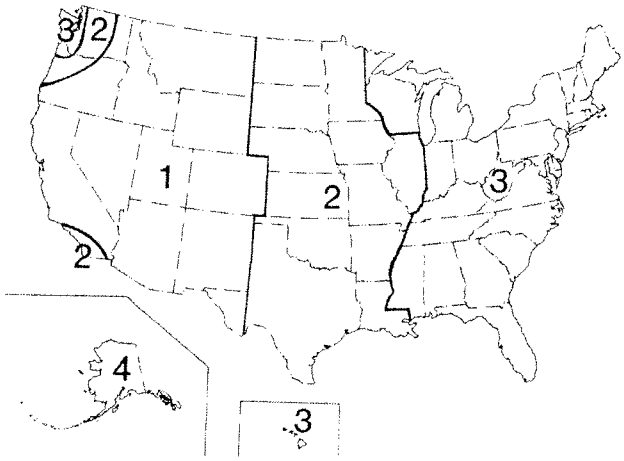

Figure 3.12.3-1 Solar Radiation Zones for the United States.

The temperature gradient given herein is a modification of that proposed in Imbsen et al. (*1985*), which was based on studies of concrete superstructures. The addition for steel superstructures is patterned after the temperature gradient for that type of bridge in the Australian bridge specifications (*AUSTROADS 1992*).

The data in Table 1 does not make a distinction regarding the presence or lack of an asphaltic overlay on decks. Field measurements have yielded apparently different indications concerning the effect of asphalt as an insulator or as a contributor (*Spring 1997*). Therefore, any possible insulating qualities have been ignored herein.

The temperatures given in Table 1 form the basis for calculating the change in temperature with depth in the cross-section, not absolute temperature.

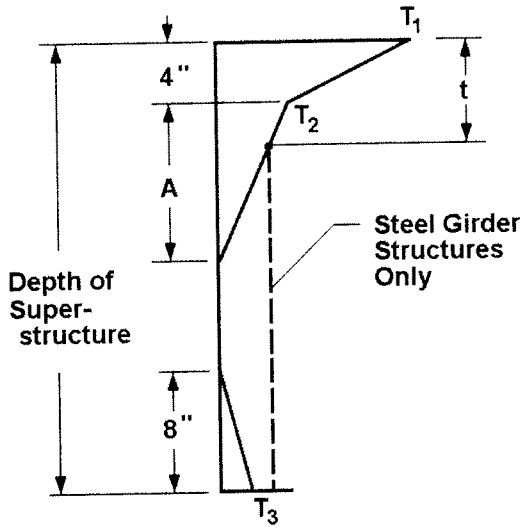

Figure 3.12.3-2 Positive Vertical Temperature Gradient in Concrete and Steel Superstructures.

3.12.4 Differential Shrinkage

Where appropriate, differential shrinkage strains between concretes of different age and composition, and between concrete and steel or wood, shall be determined in accordance with the provisions of Section 5.

C3.12.4

The Designer may specify timing and sequence of construction in order to minimize stresses due to differential shrinkage between components.

3.12.5 Creep

Creep strains for concrete and wood shall be in accordance with the provisions of Section 5 and Section 8, respectively. In determining force effects and deformations due to creep, dependence on time and changes in compressive stresses shall be taken into account.

C3.12.5

Traditionally, only creep of concrete is considered. Creep of wood is addressed only because it applies to prestressed wood decks.

3.12.6 Settlement

Force effects due to extreme values of differential settlements among substructures and within individual substructure units shall be considered. Estimates of settlement for individual substructure units may be made in accordance with the provisions in Article 10.7.2.3.

C3.12.6

Force effects due to settlement may be reduced by considering creep. Analysis for the load combinations in Tables 3.4.1-1 and 3.4.1-2 which include settlement should be repeated for settlement of each possible substructure unit settling individually, as well as combinations of substructure units settling, that could create critical force effects in the structure.

3.13 FRICTION FORCES: *FR*

Forces due to friction shall be established on the basis of extreme values of the friction coefficient between the sliding surfaces. Where appropriate, the effect of moisture and possible degradation or contamination of sliding or rotating surfaces upon the friction coefficient shall be considered.

C3.13

Low and high friction coefficients may be obtained from standard textbooks. If so warranted, the values may be determined by physical tests, especially if the surfaces are expected to be roughened in service.

3.13 FRICTION FORCES: *FR*

Forces due to friction shall be established on the basis of extreme values of the friction coefficient between the sliding surfaces. Where appropriate, the effect of moisture and possible degradation or contamination of sliding or rotating surfaces upon the friction coefficient shall be considered.

C3.13

Low and high friction coefficients may be obtained from standard textbooks. If so warranted, the values may be determined by physical tests, especially if the surfaces are expected to be roughened in service.

3.14 VESSEL COLLISION: *CV*

3.14.1 General

The provisions of this Article apply to the accidental collision between a vessel and a bridge. These provisions may be revised as stated in Article 3.14.16 to account for intentional collisions.

All bridge components in a navigable waterway crossing, located in design water depths not less than 2.0 ft., shall be designed for vessel impact.

The minimum design impact load for substructure design shall be determined using an empty hopper barge drifting at a velocity equal to the yearly mean current for the waterway location. The design barge shall be a single 35.0-ft. × 195-ft. barge, with an empty displacement of 200 ton, unless approved otherwise by the Owner.

Where bridges span deep draft waterways and are not sufficiently high to preclude contact with the vessel, the minimum superstructure design impact may be taken to be the mast collision impact load specified in Article 3.14.10.3.

C3.14.1

Intentional collision between a vessel and a bridge may be considered when conducting security studies.

The determination of the navigability of a waterway is usually made by the U.S. Coast Guard.

The requirements herein have been adapted from the AASHTO ***Guide Specifications and Commentary for Vessel Collision Design of Highway Bridges*** *(1991)* using the Method II risk acceptance alternative, **and modified for the LRFD edition (2008). The 1991 Guide Specifications required the use of a single vessel length overall (*LOA*) selected in accordance with the Method I criteria for use in estimating the geometric probability and impact speed to represent all vessel classifications. This was a conservative simplification applied to reduce the amount of effort required in the analysis. With the introduction of personal computers and programming, the simplification can be lifted and *AF* can be quickly obtained for each design vessel, which was originally envisioned. The end result is a more accurate model for the vessel collision study as well as more informative conclusions about the vessel fleet and associated probabilities of collision.**

Another source of information has been the proceedings of an international colloquium, Ship Collisions with Bridges and Offshore Structures *(IABSE, 1983)*.

Barges are categorized by ton = 2,000 lbs. and ships by tonne = 2,205 lbs.

The deadweight tonnage (DWT) of a ship is the weight of the cargo, fuel, water, and stores. The DWT is only a portion of the total vessel weight, but it gives a general estimation of the ship size.

A minimum impact requirement from an empty barge drifting in all waterways and the mast impact of a drifting ship in deep draft waterways is specified because of the high frequency of occurrences of such collision accidents in United States' waterways.

In navigable waterways where vessel collision is anticipated, structures shall be:

- Designed to resist vessel collision forces, and/or
- Adequately protected by fenders, dolphins, berms, islands, or other sacrifice-able devices.

In determining vessel collision loads, consideration shall be given to the relationship of the bridge to:

- Waterway geometry,
- Size, type, loading condition, and frequency of vessels using the waterway,
- Available water depth,
- Vessel speed and direction, and
- The structural response of the bridge to collision.

The intent of the vessel collision provisions is to minimize the risk of catastrophic failure of bridges crossing navigable waterways due to collisions by aberrant vessels. The collision impact forces represent a probabilistically based, worst-case, head-on collision, with the vessel moving in a forward direction at a relatively high velocity. The requirements are applicable to steel-hulled merchant ships larger than 1,000 DWT and to inland waterway barges.

The channel layout and geometry can affect the navigation conditions, the largest vessel size that can use the waterway and the loading condition and the speed of vessels approaching a bridge. The presence of bends, intersections with other waterways, and the presence of other bridge crossings near the bridge increase the probability of accidents. The vessel transit paths in the waterway in relation to the navigation channel and the bridge piers can affect the risk of aberrant vessels hitting the piers and the exposed portions of the superstructure.

The water level and the loading conditions of vessels influence the location on the pier where vessel impact loads are applied, and the susceptibility of the superstructure to vessel hits. **The** water depth plays a critical role in the accessibility of vessels to piers and spans outside the navigation channel. **The water depth at the pier should not include short-term scour. In addition, the water depth should not just be evaluated at the specific pier location itself, but also at locations upstream and downstream of the pier—which may be shallower and would potentially block certain deeper draft vessels from hitting the pier.** In waterways with large water stage fluctuations, the water level used can have a significant effect on the structural requirements for the pier and/or pier protection design.

The remainder of this page is intentionally left blank.

The maneuverability of ships is reduced by the low underkeel clearance typical in inland waterways. Shallow underkeel clearance can also affect the hydrodynamic forces during a collision increasing the collision energy, especially in the transverse direction. In addition, ships riding in ballast can be greatly affected by winds and currents. When under ballast, vessels are susceptible to wind gusts that could push them into the bridge.

It is very difficult to control and steer barge tows, especially near bends and in waterways with high stream velocities and cross currents. In maneuvering a bend, tows experience a sliding effect in a direction opposite to the direction of the turn, due to inertia forces which are often coupled with the current flow. Bridges located in a high velocity waterway and near a bend in the channel will probably be hit by barges at frequent intervals.

Unless otherwise indicated in these Specifications, an evaluation of the following two vessel collision events combined with scour conditions are recommended:

- **A drifting empty barge breaking loose from its moorings and striking the bridge. The vessel impact loads should be combined with one-half of the predicted long-term scour plus one-half of the predicted short term scour. The flow rate, water level, and short-term scour depth are those associated with the design flood for bridge scour (100-year flood event).**

A ship or barge tow striking the bridge while transiting the navigation channel under typical waterway conditions. The vessel impact loads should be combined with the effects of one-half of the long-term scour and no short-term scour. The flow rate and water level should be taken as the yearly mean conditions.

3.14.2 Owner's Responsibility

The Owner shall establish and/or approve the bridge **operational** classification, the vessel traffic density in the waterway, and the design velocity of vessels for the bridge. The Owner shall specify or approve the degree of damage that the bridge components, including protective systems, are allowed to sustain.

C3.14.2

Pier protection systems may also be warranted for bridges over navigable channels transversed only by pleasure boats or small commercial vessels. For such locations, dolphins and fender systems are commonly used to protect the pier and to minimize the hazards of passage under the bridge for the vessels using the waterway.

3.14.3 Operational Classification

For the purpose of Article 3.14, an **operational** classification, either "critical **or essential**" or "**typical**," shall be determined for all bridges located in navigable waterways. Critical bridges shall continue to function after an impact, the probability of which is smaller than regular bridges.

C3.14.3

This Article implies that a critical **or essential** bridge may be damaged to an extent acceptable to the Owner, as specified in Article 3.14.2, but should not collapse and should remain serviceable, even though repairs are needed.

3.14.4 Design Vessel

A design vessel for each pier or span component shall be selected, such that the estimated annual frequency of collapse computed in accordance with Article 3.14.5, due to vessels not smaller than the design vessel, is less than the acceptance criterion for the component.

The design vessels shall be selected on the basis of the bridge **operational** classification and the vessel, bridge, and waterway characteristics.

C3.14.4

An analysis of the annual frequency of collapse is performed for each pier or span component exposed to collision. From this analysis, a design vessel and its associated collision loads can be determined for each pier or span component. The design vessel size and impact loads can vary greatly among the components of the same structure, depending upon the waterway geometry, available water depth, bridge geometry, and vessel traffic characteristics.

The design vessel is selected using a probability-based analysis procedure in which the predicted annual frequency of bridge collapse, AF, is compared to an acceptance criterion. The analysis procedure is an iterative process in which a trial design vessel is selected for a bridge component and a resulting AF is computed using the characteristics of waterway, bridge, and vessel fleet. This AF is compared to the acceptance criterion, and revisions to the analysis variables are made as necessary to achieve compliance. The primary variables that the Designer can usually alter include the:

- Location of the bridge in the waterway,
- Location and clearances of bridge pier and span components,
- Resistance of piers and superstructures, and
- Use of protective systems to either reduce or eliminate the collision forces.

3.14.5 Annual Frequency of Collapse

The annual frequency of a bridge component collapse shall be taken as:

$$AF = (N)(PA)(PG)(PC)(PF) \qquad \textbf{(3.14.5-1)}$$

where:

AF = annual frequency of bridge component collapse due to vessel collision

N = the annual number of vessels, classified by type, size, and loading condition, that utilize the channel

PA = the probability of vessel aberrancy

PG = the geometric probability of a collision between an aberrant vessel and a bridge pier or span

PC = the probability of bridge collapse due to a collision with an aberrant vessel

PF = **adjustment factor to account for potential protection of the piers from vessel collision due to upstream or downstream land masses or other structures that block the vessel**

AF shall be computed for each bridge component and vessel classification. The annual frequency of collapse for the total bridge shall be taken as the sum of all component AFs.

For critical **or essential** bridges, the maximum annual frequency of collapse, AF, for the whole bridge, shall be taken as 0.0001.

For **typical** bridges, the maximum annual frequency of collapse, AF, for the total bridge, shall be taken as 0.001.

C3.14.5

Various types of risk assessment models have been developed for vessel collision with bridges by researchers worldwide (*IABSE 1983; Modjeski and Masters 1984; Prucz 1987; Larsen 1993*). Practically all of these models are based on a form similar to Eq. 1, which is used to compute the annual frequency of bridge collapse, AF, associated with a particular bridge component.

The inverse of the annual frequency of collapse, $1/AF$, is equal to the return period in years. The summation of AFs computed over all of the vessel classification intervals for a specific component equals the annual frequency of collapse of the component.

Risk can be defined as the potential realization of unwanted consequences of an event. Both a probability of occurrence of an event and the magnitude of its consequences are involved. Defining an acceptable level of risk is a value-oriented process and is by nature subjective (*Rowe 1977*).

For waterways with widths less than 6.0 times the length overall of the design vessel, *LOA*, the acceptance criterion for the annual frequency of collapse for each pier and superstructure component shall be determined by distributing the total bridge acceptance criterion, *AF*, over the number of pier and span components located in the waterway.

For wide waterways with widths greater than 6.0 times *LOA*, the acceptance criterion for the annual frequency of collapse for each pier and span component shall be determined by distributing the total bridge acceptance criterion over the number of pier and superstructure components located within the distance 3.0 times *LOA* on each side of the inbound and outbound vessel transit centerline paths.

Based on historical collision data, the primary area of concern for vessel impact is the central portion of the bridge near the navigation channel. The limits of this area extend to a distance of 3.0 times *LOA* on each side of the inbound and outbound vessel transit path centerlines. For most bridges, these vessel transit path centerlines coincide with the centerline of the navigable channel. Where two-way vessel traffic exists under the bridge, the vessel transit path centerline of the inbound and outbound vessels should be taken as the centerline of each half of the channel, respectively.

The distribution of the *AF* acceptance criterion among the exposed pier and span components is based on the Designer's judgment. One method is to equally spread the acceptable risk among all the components. This method is usually not desirable because it fails to take into account the importance and higher cost of most main span components. The preferred method is to apportion the risk to each pier and span component on the basis of its percentage value to the replacement cost of the structure in the central analysis area.

3.14.5.1 Vessel Frequency Distribution

The number of vessels, *N*, based on size, type, and loading condition and available water depth shall be developed for each pier and span component to be evaluated. Depending on waterway conditions, a differentiation between the number and loading condition of vessels transiting inbound and outbound shall be considered.

C3.14.5.1

In developing the design vessel distribution, the Designer should first establish the number and characteristics of the vessels using the navigable waterway or channel under the bridge. Because the water depth limits the size of vessel that could strike a bridge component, the navigable channel vessel frequency data can be modified, as required, on the basis of the water depth at each bridge component to determine the number and characteristics of the vessels that could strike the pier or span component being analyzed. Thus, each component could have a different value of *N*.

Vessel characteristics necessary to conduct the analysis include:

- Type, i.e., ship or barge;
- Size based on the vessel's deadweight tonnage, *DWT*;
- Inbound and outbound operating characteristics;
- Loading condition, i.e., loaded, partly loaded, ballasted, or empty;
- Length overall, *LOA*;
- Width or beam, B_M;
- Draft associated with each loading condition;
- Bow depth, D_B;

- Bow shape;
- Displacement tonnage, W;
- Vertical clearances; and
- Number of transits under the bridge each year.

Sources for the vessel data and typical ship and barge characteristics are included in the AASHTO *Guide Specifications and Commentary for Vessel Collision Design of Highway Bridges (1991)*.

The Designer should use judgment in developing a distribution of the vessel frequency data based on discrete groupings or categories of vessel size by *DWT*. It is recommended that the *DWT* intervals used in developing the vessel distribution not exceed 20,000 DWT for vessels smaller than 100,000 DWT, and not exceeding 50,000 DWT for ships larger than 100,000 DWT.

3.14.5.2 Probability of Aberrancy

3.14.5.2.1 General

The probability of vessel aberrancy, *PA*, may be determined by the statistical or the approximate method.

C3.14.5.2.1

The probability of aberrancy is mainly related to the navigation conditions at the bridge site. Vessel traffic regulations, vessel traffic management systems and aids to navigation can improve the navigation conditions and reduce the probability of aberrancy.

The probability of aberrancy, *PA*, sometimes referred to as the causation probability, is a measure of the risk that a vessel is in trouble as a result of pilot error, adverse environmental conditions, or mechanical failure.

An evaluation of accident statistics indicates that human error and adverse environmental conditions, not mechanical failures, are the primary reasons for accidents. In the United States, an estimated 60 percent to 85 percent of all vessel accidents have been attributed to human error.

3.14.5.2.2 Statistical Method

The probability of aberrancy may be computed on the basis of a statistical analysis of historical data on vessel collisions, rammings, and groundings in the waterway and on the number of vessels transiting the waterway during the period of accident reporting.

C3.14.5.2.2

The most accurate procedure for determining *PA* is to compute it using long-term vessel accident statistics in the waterway and data on the frequency of ship/barge traffic in the waterway during the same period of time (*Larsen 1983*). Data from ship simulation studies and radar analysis of vessel movements in the waterway have also been used to estimate *PA*. Based on historical data, it has been determined that the aberrancy rate for barges is usually two to three times that measured for ships in the same waterway.

3.14.5.2.3 Approximate Method

The probability of aberrancy may be taken as:

$$PA = (BR)(R_B)(R_C)(R_{XC})(R_D) \qquad (3.14.5.2.3\text{-}1)$$

where:

PA = probability of aberrancy

BR = aberrancy base rate

R_B = correction factor for bridge location

R_C = correction factor for current acting parallel to vessel transit path

R_{XC} = correction factor for cross-currents acting perpendicular to vessel transit path

R_D = correction factor for vessel traffic density

The base rate, BR, of aberrancy shall be taken as:

- For ships:

$$BR = 0.6 \times 10^{-4}$$

- For barges:

$$BR = 1.2 \times 10^{-4}$$

The correction factor for bridge location, R_B, based on the relative location of the bridge in either of three waterway regions, as shown in Figure 1, shall be taken as:

- For straight regions:

$$R_B = 1.0 \qquad (3.14.5.2.3\text{-}2)$$

- For transition regions:

$$R_B = \left(1 + \frac{\theta}{90^\circ}\right) \qquad (3.14.5.2.3\text{-}3)$$

- For turn/bend regions:

$$R_B = \left(1 + \frac{\theta}{45^\circ}\right) \qquad (3.14.5.2.3\text{-}4)$$

where:

θ = angle of the turn or bend specified in Figure 1 (°)

C3.14.5.2.3

Because the determination of PA based on actual accident data in the waterway is often a difficult and time-consuming process, an alternative method for estimating PA was established during the development of the AASHTO *Guide Specification on Vessel Collision Design of Highway Bridges*. The equations in this Article are empirical relationships based on historical accident data. The predicted PA value using these equations and the values determined from accident statistics are generally in agreement, although exceptions do occur.

It should be noted that the procedure for computing PA using Eq. 1 should not be considered to be either rigorous or exhaustive. Several influences, such as wind, visibility conditions, navigation aids, pilotage, etc., were not directly included in the method because their effects were difficult to quantify. These influences have been indirectly included because the empirical equations were developed from accident data in which these factors had a part.

It is anticipated that future research will provide a better understanding of the probability of aberrancy and how to accurately estimate its value. The implementation of advanced vessel traffic control systems using automated surveillance and warning technology should significantly reduce the probability of aberrancy in navigable waterways.

The correction factor, R_C, for currents acting parallel to the vessel transit path in the waterway shall be taken as:

$$R_C = \left(1 + \frac{V_C}{10} \right) \qquad (3.14.5.2.3\text{-}5)$$

where:

V_C = current velocity component parallel to the vessel transit path (knots)

The correction factor, R_{XC}, for cross-currents acting perpendicular to the vessel transit path in the waterway shall be taken as:

$$R_{XC} = (1 + V_{XC}) \qquad (3.14.5.2.3\text{-}6)$$

where:

V_{XC} = current velocity component perpendicular to the vessel transit path (knots)

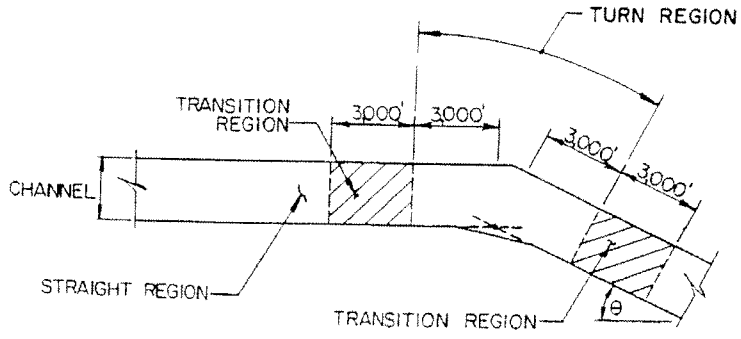

a. Turn in Channel

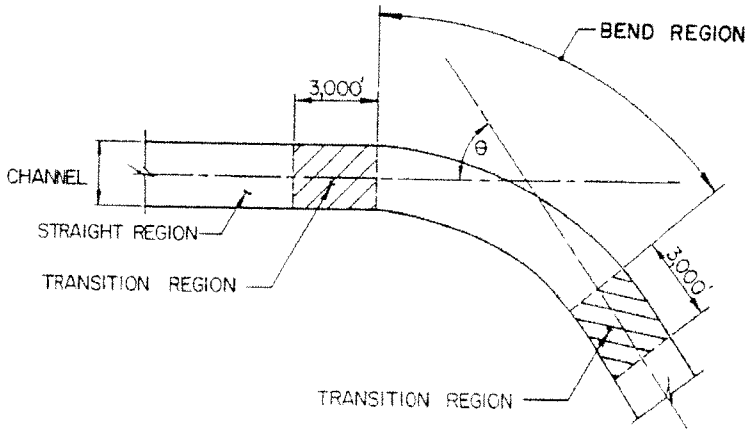

b. Bend in Channel

Figure 3.14.5.2.3-1 Waterway Regions for Bridge Location.

The correction factor for vessel traffic density, R_D, shall be selected on the basis of the ship/barge traffic density level in the waterway in the immediate vicinity of the bridge defined as:

- Low density—vessels rarely meet, pass, or overtake each other in the immediate vicinity of the bridge:

$$R_D = 1.0 \qquad (3.14.5.2.3\text{-}7)$$

- Average density—vessels occasionally meet, pass, or overtake each other in the immediate vicinity of the bridge:

$$R_D = 1.3 \qquad (3.14.5.2.3\text{-}8)$$

- High density—vessels routinely meet, pass, or overtake each other in the immediate vicinity of the bridge:

$$R_D = 1.6 \qquad (3.14.5.2.3\text{-}9)$$

3.14.5.3 Geometric Probability

A normal distribution may be utilized to model the sailing path of an aberrant vessel near the bridge. The geometric probability, *PG*, shall be taken as the area under the normal distribution bounded by the pier width and the width of the vessel on each side of the pier, as specified in Figure 1. The standard deviation, σ, of the normal distribution shall be assumed to be equal to the length overall, *LOA*, of the design vessel selected in accordance with Article 3.14.4.

The location of the mean of the standard distribution shall be taken at the centerline of the vessel transit path. *PG* shall be determined based on the width, B_M, of each vessel classification category, or it may be determined for all classification intervals using the B_M of the design vessel selected in accordance with Article 3.14.4.

C3.14.5.3

The geometric probability, *PG*, is defined as the conditional probability that a vessel will hit a bridge pier or superstructure component, given that it has lost control, i.e., it is aberrant, in the vicinity of the bridge. The probability of occurrence depends on the following factors:

- Geometry of waterway;
- Water depths of waterway;
- Location of bridge piers;
- Span clearances;

Sailing path of vessel;

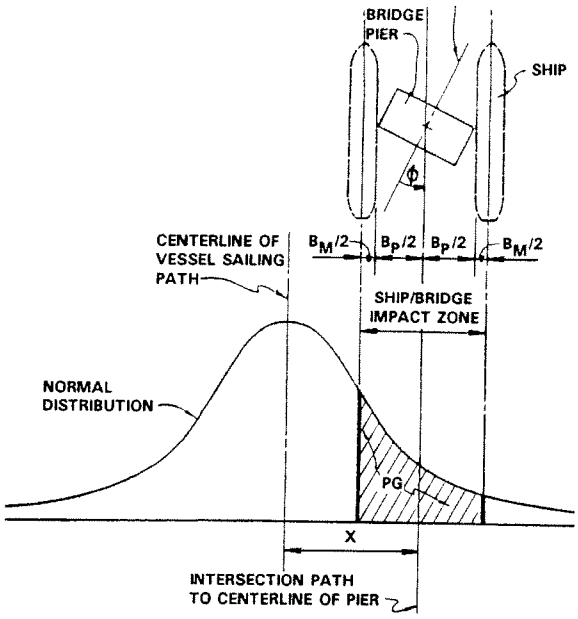

Figure 3.14.5.3-1 Geometric Probability of Pier Collision.

- Maneuvering characteristics of vessel;
- Location, heading, and velocity of vessel;
- Rudder angle at time of failure;
- Environmental conditions;
- Width, length, and shape of vessel; and
- Vessel draft.

The horizontal clearance of the navigation span has a significant impact on the risk of vessel collision with the main piers. Analysis of past collision accidents has shown that fixed bridges with a main span less than two to three times the design vessel length or less than two times the channel width are particularly vulnerable to vessel collision.

Various geometric probability models, some based on simulation studies, have been recommended and used on different bridge projects and for the development of general design provisions. Descriptions of these models may be found in IABSE (*1983*), Modjeski and Masters (*1984*), Prucz (*1987*), and Larsen (*1993*). The method used to determine *PG* herein is similar to that proposed by Knott et al. (*1985*). The use of a normal distribution is based on historical ship/bridge accident data. It is recommended that $\sigma = LOA$ of the design vessel for computing *PG*, and that bridge components located beyond 3σ from the centerline of the vessel transit path not be included in the analysis, other than the minimum impact requirement of Article 3.14.1.

The accident data used to develop the *PG* methodology primarily represents ships. Although barge accidents occur relatively frequently in United States waterways, there have been little published research findings concerning the distribution of barge accidents over a waterway. Until such data and research become available, it is recommended that the same $\sigma = LOA$ developed for ships be applied to barges with the barge *LOA* equal to the total length of the barge tow, including the towboat.

3.14.5.4 Probability of Collapse

The probability of bridge collapse, *PC*, based on the ratio of the ultimate lateral resistance of the pier, H_P, and span, H_S, to the vessel impact force, *P*, shall be taken as:

- If $0.0 \le H/P < 0.1$, then

$$PC = 0.1 + 9\left(0.1 - \frac{H}{P}\right) \qquad (3.14.5.4\text{-}1)$$

- If $0.1 \le H/P < 1.0$, then

$$PC = 0.111\left(1 - \frac{H}{P}\right) \qquad (3.14.5.4\text{-}2)$$

C3.14.5.4

The probability that the bridge will collapse once it has been struck by an aberrant vessel, *PC*, is complex and is a function of the vessel size, type, configuration, speed, direction, and mass. It is also dependent on the nature of the collision and stiffness/strength characteristic of the bridge pier and superstructure to resist the collision impact loads.

The methodology for estimating *PC* was developed by Cowiconsult (*1987*) from studies performed by Fujii and Shiobara (*1978*) using Japanese historical damage data on vessels colliding at sea. The damage to bridge piers is based on ship damage data because accurate damage data for collision with bridges is relatively scarce.

- If $H/P \geq 1.0$, then

$$PC = 0.0 \qquad (3.14.5.4\text{-}3)$$

where:

PC = probability of collapse

H = resistance of bridge component to a horizontal force expressed as pier resistance, H_P, or superstructure resistance, H_S (kip)

P = vessel impact force, P_S, P_{BH}, P_{DH}, or P_{MT}, specified in Articles 3.14.8, 3.14.10.1, 3.14.10.2, and 3.14.10.3, respectively (kip)

Figure C1 is a plot of the probability of collapse relationships. From this figure, the following results are evident:

- Where the pier or superstructure impact resistance exceeds the vessel collision impact force of the design vessel, the bridge collapse probability becomes 0.0.
- Where the pier or superstructure impact resistance is in the range 10 to 100 percent of the collision force of the design vessel, the bridge collapse probability varies linearly between 0.0 and 0.10.
- Where the pier or superstructure impact resistance is below 10 percent of the collision force, the bridge collapse probability varies linearly between 0.10 and 1.0.

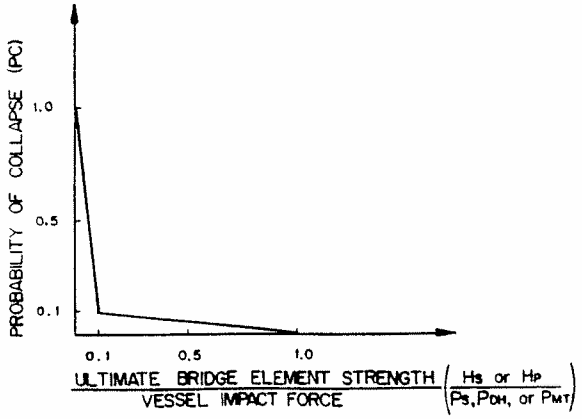

Figure C3.14.5.4-1 Probability of Collapse Distribution.

3.14.5.5 Protection Factor

The protection factor, *PF*, shall be computed as:

$$PF = 1 - (\%\ \text{Protection Provided}/100) \qquad \textbf{(3.14.5.5-1)}$$

If no protection of the pier exists, then $PF = 1.0$. If the pier is 100 percent protected, then $PF = 0.0$. If the pier protection (for example, a dolphin system) provides 70 percent protection, then *PF* would be equal to 0.3. Values for *PF* may vary from pier to pier and may vary depending on the direction of the vessel traffic (i.e., vessel traffic moving inbound versus traffic moving outbound).

C3.14.5.5

The purpose of the protection factor, *PF*, is to adjust the annual frequency of collapse, *AF*, for full or partial protection of selected bridge piers from vessel collisions such as:

- **Dolphins, islands, etc.,**
- **Existing site conditions such as a parallel bridge protecting a bridge from impacts in one direction,**
- **A feature of the waterway (such as a peninsula extending out on one side of the bridge) that may block vessels from hitting bridge piers, or**
- **A wharf structure near the bridge that may block vessels from a certain direction.**

The recommended procedure for estimating values for *PF* is shown in Figure C1. It illustrates a simple model developed to estimate the effectiveness of dolphin protection on a bridge pier.

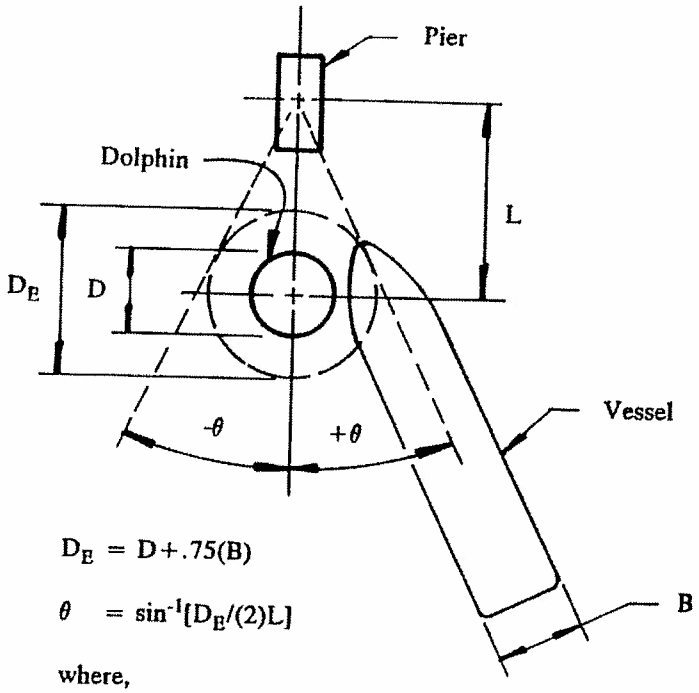

$D_E = D+.75(B)$

$\theta = \sin^{-1}[D_E/(2)L]$

where,

θ = Protection angle provided by dolphin
D = Diameter of dolphin (ft)
B = Beam (width) of vessel (ft)
L = Distance of dolphin from pier (ft)
D_E = Effective dolphin diameter (ft)

a. Plan of Dolphin Protection.

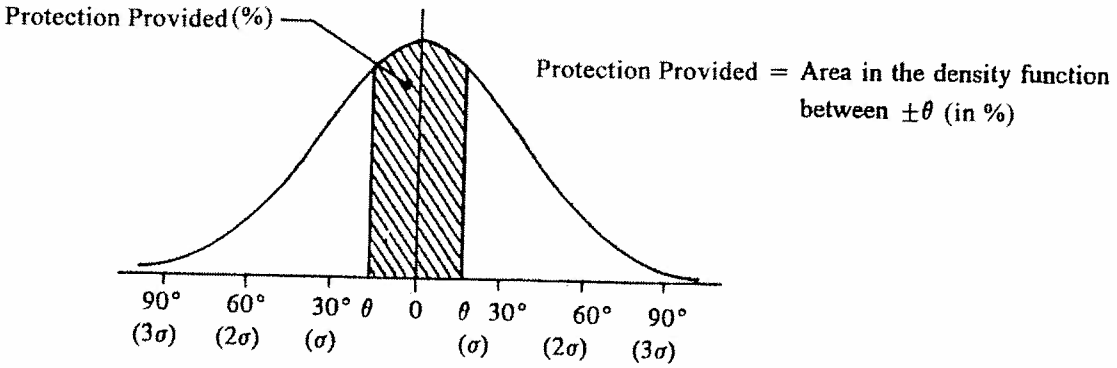

b. Normal Distribution of Vessel Collision Trajectories Around Bridge Pier (σ assumed = 30°).

Figure C3.14.5.5-1 Illustrative Model of the Protection Factor (*PF*) of Dolphin Protection around a Bridge Pier.

3.14.6 Design Collision Velocity

The design collision velocity may be determined as specified in Figure 1, for which:

V = design impact velocity (ft./sec.)

V_T = typical vessel transit velocity in the channel under normal environmental conditions but not taken to be less than V_{MIN} (ft./sec.)

V_{MIN} = minimum design impact velocity taken as not less than the yearly mean current velocity for the bridge location (ft./sec.)

C3.14.6

A triangular distribution of collision impact velocity across the length of the bridge and centered on the centerline of the vessel transit path in the channel was based on historical accident data. This data indicated that aberrant ships and barges that collide with bridge piers further away from the channel are moving at reduced velocities compared with those hitting piers located closer to the navigable channel limits. Aberrant vessels located at long distances from the channel are usually drifting with the current. Aberrant vessels, located very near the channel, are moving at velocities approaching that of ships and barges in the main navigation channel.

X = distance to face of pier from centerline of channel (ft.)

X_C = distance to edge of channel (ft.)

X_L = distance equal to 3.0 times the length overall of the design vessel (ft.)

The length overall, *LOA*, for barge tows shall be taken as the total length of the tow plus the length of the tug/tow boat.

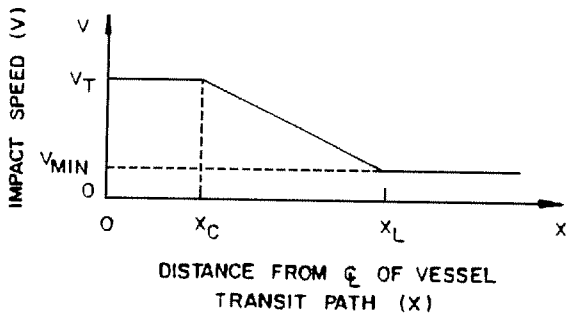

Figure 3.14.6-1 Design Collision Velocity Distribution.

The exact distribution of the velocity reduction is unknown. However, a triangular distribution was chosen because of its simplicity as well as its reasonableness in modeling the aberrant vessel velocity situation. The use of the distance 3.0 times *LOA* in Figure 1 to define the limits at which the design velocity becomes equal to that of the water current was based on the observation that very few accidents, other than with drifting vessels, have historically occurred beyond that boundary.

The selection of the design collision velocity is one of the most significant design parameters associated with the vessel collision requirements. Judgment should be exercised in determining the appropriate design velocity for a vessel transiting the waterway. The chosen velocity should reflect the "typical" transit velocity of the design vessel under "typical" conditions of wind, current, visibility, opposing traffic, waterway geometry, etc. A different vessel velocity may be required for inbound vessels than for outbound vessels given the presence of currents that may exist in the waterway.

In waterways subject to seasonal flooding, consideration should be given to flood flow velocities in determining the minimum collision velocity.

In general, the design velocity should not be based on extreme values representing extreme events, such as exceptional flooding and other extreme environmental conditions. Vessels transiting under these conditions are not representative of the "annual average" situations reflecting the typical transit conditions.

3.14.7 Vessel Collision Energy

The kinetic energy of a moving vessel to be absorbed during a noneccentric collision with a bridge pier shall be taken as:

$$KE = \frac{C_H W V^2}{29.2} \qquad (3.14.7\text{-}1)$$

where:

KE = vessel collision energy (kip-ft.)

W = vessel displacement tonnage (tonne)

C_H = hydrodynamic mass coefficient

V = vessel impact velocity (ft./sec.)

C3.14.7

Eq. 1 is the standard $mV^2/2$ relationship for computing kinetic energy with conversion from mass to weight, conversion of units and incorporation of a hydrodynamic mass coefficient, C_H, to account for the influence of the surrounding water upon the moving vessel. Recommendations for estimating C_H for vessels moving in a forward direction were based on studies by Saul and Svensson (*1980*) and data published by PIANC (*1984*). It should be noted that these hydrodynamic mass coefficients are smaller than those normally used for ship berthing computations, in which a relatively large mass of water moves with the vessel as it approaches a dock from a lateral, or broadside, direction.

The vessel displacement tonnage, W, shall be based upon the loading condition of the vessel and shall include the empty weight of the vessel, plus consideration of the weight of cargo, DWT, for loaded vessels, or the weight of water ballast for vessels transiting in an empty or lightly loaded condition. The displacement tonnage for barge tows shall be the sum of the displacement of the tug/tow vessel and the combined displacement of a row of barges in the length of the tow.

The hydrodynamic mass coefficient, C_H, shall be taken as:

- If underkeel clearance exceeds 0.5 × draft:

$$C_H = 1.05 \qquad (3.14.7\text{-}2)$$

- If underkeel clearance is less than 0.1 × draft:

$$C_H = 1.25 \qquad (3.14.7\text{-}3)$$

Values of C_H may be interpolated from the range shown above for intermediate values of underkeel clearance. The underkeel clearance shall be taken as the distance between the bottom of the vessel and the bottom of the waterway.

3.14.8 Ship Collision Force on Pier

The head-on ship collision impact force on a pier shall be taken as:

$$P_S = 8.15 V \sqrt{DWT} \qquad (3.14.8\text{-}1)$$

where:

P_S = equivalent static vessel impact force (kip)

DWT = deadweight tonnage of vessel (tonne)

V = vessel impact velocity (ft./sec.)

C3.14.8

The determination of the impact load on a bridge structure during a ship collision is complex and depends on many factors as follows:

- Structural type and shape of the ship's bow,
- Degree of water ballast carried in the forepeak of the bow,
- Size and velocity of the ship,
- Geometry of the collision, and
- Geometry and strength characteristics of the pier.

Eq. 1 was developed from research conducted by Woisin (*1976*) in West Germany to generate collision data with a view to protecting the reactors of nuclear-powered ships from collisions with other ships. The ship collision data resulted from collision tests with physical ship models at scales of 1:12.0 and 1:7.5. Woisin's results have been found to be in good agreement with the results of research conducted by other ship collision investigators worldwide (*IABSE 1983*).

Figure C1 indicates the scatter in Woisin's test data due to the various collision factors discussed herein, the triangular probability density function used to model the scatter, and the selection of a 70 percent fractile force for use as an equivalent static impact force for bridge design. Using a 70 percent fractile force for a given design vessel, the number of smaller ships with a crushing strength greater than this force would be approximately equal to the number of larger ships with a crushing strength less than this force. Figure C2 indicates typical ship impact forces computed with Eq. 1.

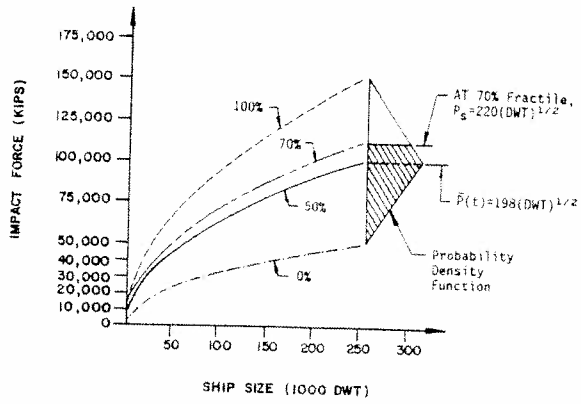

Figure C3.14.8-1 Probability Density Function of Ship Impact Force Data.

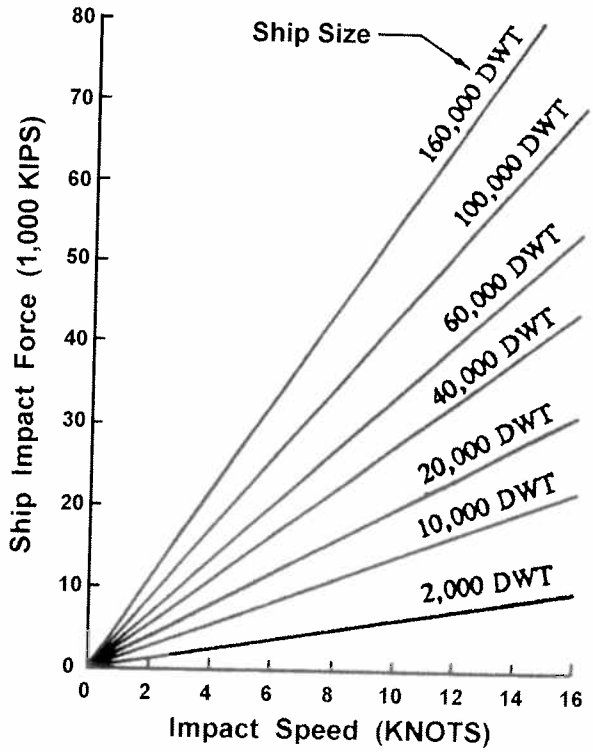

Figure C3.14.8-2 Typical Ship Impact Forces.

3.14.9 Ship Bow Damage Length

The horizontal length of the ship's bow, crushed by impact with a rigid object, shall be taken as:

$$a_S = 1.54\left(\frac{KE}{P_S}\right) \qquad (3.14.9\text{-}1)$$

where:

a_s = bow damage length of ship (ft.)

KE = vessel collision energy (kip-ft.)

P_S = ship impact force as specified in Eq. 3.14.8-1 (kip)

C3.14.9

The average bow damage length, a, is computed based on the impact force averaged against the work path, $P(a)$, such that:

$$a = \frac{KE}{P(a)} \qquad (C3.14.9\text{-}1)$$

The 1.54 coefficient used to compute the design ship damage depth in Eq. 1 results from the multiplication of the following factors:

- 1.25 to account for the increase in average impact force over time versus damage length,
- 1.11 to account for the increase in average impact force to the 70 percent design fractile, and
- 1.11 to provide an increase in the damage length to provide a similar level of design safety as that used to compute P_S.

3.14.10 Ship Collision Force on Superstructure

3.14.10.1 Collision with Bow

The bow collision impact force on a superstructure shall be taken as:

$$P_{BH} = (R_{BH})(P_S) \qquad (3.14.10.1\text{-}1)$$

where:

P_{BH} = ship bow impact force on an exposed superstructure (kip)

R_{BH} = ratio of exposed superstructure depth to the total bow depth

P_S = ship impact force specified in Eq. 3.14.8-1 (kip)

For the purpose of this Article, exposure is the vertical overlap between the vessel and the bridge superstructure with the depth of the impact zone.

C3.14.10.1

Limited data exists on the collision forces between ship bows and bridge superstructure components.

3.14.10.2 Collision with Deck House

The deck house collision impact force on a superstructure shall be taken as:

$$P_{DH} = (R_{DH})(P_S) \qquad (3.14.10.2\text{-}1)$$

where:

P_{DH} = ship deck house impact force (kip)

R_{DH} = reduction factor specified herein

P_S = ship impact force as specified in Eq. 3.14.8-1 (kip)

For ships exceeding 100,000 tonne, R_{DH} shall be taken as 0.10. For ships smaller than 100,000 tonne:

$$R_{DH} = 0.2 - \left(\frac{DWT}{100{,}000}\right)(0.10) \qquad (3.14.10.2\text{-}2)$$

3.14.10.3 Collision with Mast

The mast collision impact force on a superstructure shall be taken as:

$$P_{MT} = 0.10P_{DH} \qquad (3.14.10.3\text{-}1)$$

where:

P_{MT} = ship mast impact force (kip)

P_{DH} = ship deck house impact force specified in Eq. 3.14.10.2-1 (kip)

3.14.11 Barge Collision Force on Pier

For the purpose of Article 3.14, the standard hopper barge shall be taken as an inland river barge with:

width	=	35.0 ft.
length	=	195.0 ft.
depth	=	12.0 ft.
empty draft	=	1.7 ft.
loaded draft	=	8.7 ft.
DWT	=	1,700 tons

The collision impact force on a pier for a standard hopper barge shall be taken as:

- If $a_B < 0.34$ then:

$$P_B = 4{,}112a_B \qquad (3.14.11\text{-}1)$$

C3.14.10.2

According to the Great Belt Bridge investigation in Denmark (*Cowiconsult, Inc. 1981*) forces for deck house collision with a bridge superstructure:

P_{DH} = 1,200 kip for the deck house collision of a 1,000 DWT freighter ship, and

P_{DH} = 6,000 kip for the deck house collision of a 100,000 DWT tanker ship.

Based on these values, the approximate empirical relationship of Eq. 1 was developed for selecting superstructure design impact values for deck house collision.

C3.14.10.3

Eq. 1 was developed by estimating the impact forces based on bridge girder and superstructure damage from a limited number of mast impact accidents.

C3.14.11

There is less reported data on impact forces resulting from barge collisions than from ship collision. The barge collision impact forces determined by Eqs. 1 and 2 were developed from research conducted by Meir-Dornberg (*1983*) in West Germany. Meir-Dornberg's study included dynamic loading with a pendulum hammer on barge bottom models in scale 1:4.5, static loading on one bottom model in scale 1:6, and numerical analysis. The results for the standard European Barge, Type IIa, which has a similar bow to the standard hopper barge in the United States, are shown in Figure C1 for barge deformation and impact loading. No significant difference was found between the static and dynamic forces measured during the study. Typical barge tow impact forces using Eqs. 1 and 2 are shown in Figure C2.

- If $a_B \geq 0.34$ then:

$$P_B = 1{,}349 + 110a_B \qquad (3.14.11\text{-}2)$$

where:

P_B = equivalent static barge impact force (kip)

a_B = barge bow damage length specified in Eq. 3.14.12-1 (ft.)

The impact force for design barges larger than the standard hopper barge shall be determined by increasing the standard hopper barge impact force by the ratio of the larger barge's width to the width of the standard hopper barge.

where:

E_B = deformation energy (kip-ft.)

$\overline{P_B}$ = average equivalent static barge impact force resulting from the study (kip)

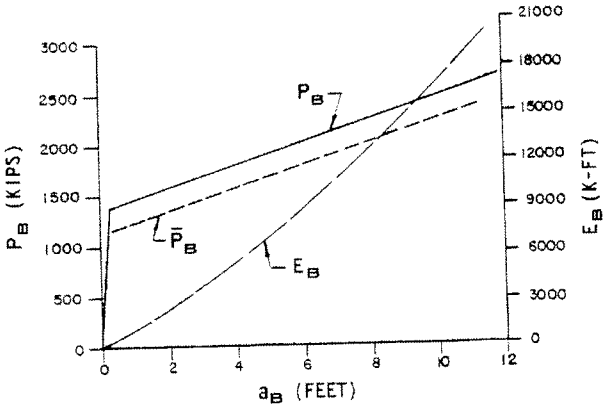

Figure C3.14.11-1 Barge Impact Force, Deformation Energy, and Damage Length Data.

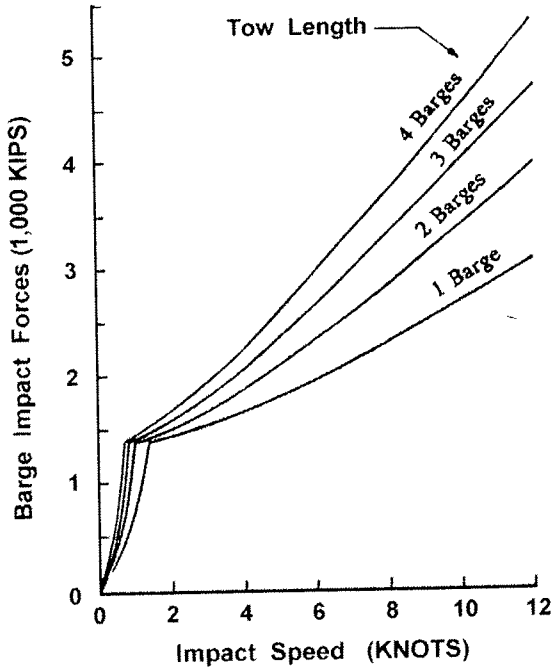

Figure C3.14.11-2 Typical Hopper Barge Impact Forces.

3.14.12 Barge Bow Damage Length

The barge bow horizontal damage length for a standard hopper barge shall be taken as:

$$a_B = 10.2\left(\sqrt{1+\frac{KE}{5,672}}-1\right) \qquad (3.14.12\text{-}1)$$

where:

a_B = barge bow damage length (ft.)

KE = vessel collision energy (kip-ft.)

C3.14.12

The relationship for barge horizontal damage length, a_B, was developed from the same research conducted on barge collisions by Meir-Dornberg, as discussed in Article C3.14.11.

3.14.13 Damage at the Extreme Limit State

Inelastic behavior and redistribution of force effects is permitted in substructure and superstructure components, provided that sufficient ductility and redundancy of the remaining structure exists in the extreme event limit state to prevent catastrophic superstructure collapse.

As an alternative, pier protection may be provided for the bridge structure to eliminate or reduce the vessel collision loads applied to the bridge structure to acceptable levels.

C3.14.13

Two basic protection options are available to the Bridge Designer. The first option involves designing the bridge to withstand the impact loads in either an elastic or inelastic manner. If the response to collision is inelastic, the design must incorporate redundancy or other means to prevent collapse of the superstructure.

The second option is to provide a protective system of fenders, pile-supported structures, dolphins, islands, etc., either to reduce the magnitude of the impact loads to less than the strength of the bridge pier or superstructure components or to independently protect those components.

The requirements for either of these two options are general in nature because the actual design procedures that could be used vary considerably. This is particularly true for inelastic design. Because little information is available on the behavior of the inelastic deformation of materials and structures during the type of dynamic impacts associated with vessel impact, assumptions based on experience and sound engineering practice should be substituted.

3.14.14 Application of Impact Force

3.14.14.1 Substructure Design

For substructure design, equivalent static forces, parallel and normal to the centerline of the navigable channel, shall be applied separately as follows:

- 100 percent of the design impact force in a direction parallel to the alignment of the center-line of the navigable channel, or
- 50 percent of the design impact force in the direction normal to the direction of the centerline of the channel.

C3.14.14.1

All components of the substructure, exposed to physical contact by any portion of the design vessel's hull or bow, shall be designed to resist the applied loads. The bow overhang, rake, or flair distance of ships and barges shall be considered in determining the portions of the substructure exposed to contact by the vessel. Crushing of the vessel's bow causing contact with any setback portion of the substructure shall also be considered.

The impact force in both design cases, specified herein, shall be applied to a substructure in accordance with the following criteria:

- For overall stability, the design impact force is applied as a concentrated force on the substructure at the mean high water level of the waterway, as shown in Figure 1, and

- For local collision forces, the design impact force is applied as a vertical line load equally distributed along the ship's bow depth, as shown in Figure 2. The ship's bow is considered to be raked forward in determining the potential contact area of the impact force on the substructure. For barge impact, the local collision force is taken as a vertical line load equally distributed on the depth of the head block, as shown in Figure 3.

Two cases should be evaluated in designing the bridge substructure for vessel impact loadings:

- The overall stability of the substructure and foundation, assuming that the vessel impact acts as a concentrated force at the waterline, and

- The ability of each component of the substructure to withstand any local collision force resulting from a vessel impact.

The need to apply local collision forces on substructures exposed to contact by overhanging portions of a ship or barge's bow is well documented by accident case histories. The Sunshine Skyway Bridge in Tampa Bay, Florida, collapsed in 1980 as a result of the ship's bow impacting a pier column at a point 42.0 ft. above the waterline. Ship and barge bow rake lengths are often large enough that they can even extend over protective fender systems and contact vulnerable bridge components, as shown in Figures C1 and C2. Bow shapes and dimensions vary widely, and the Designer may need to perform special studies to establish vessel bow geometry for a particular waterway location. Typical bow geometry data is provided in AASHTO (*1991*).

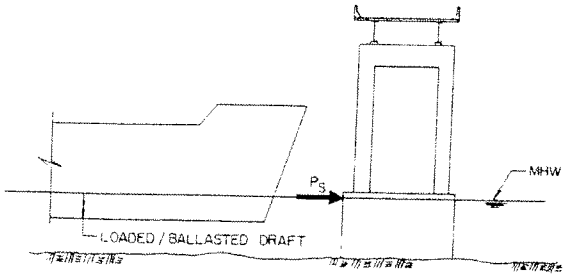

Figure 3.14.14.1-1 Ship Impact Concentrated Force on Pier.

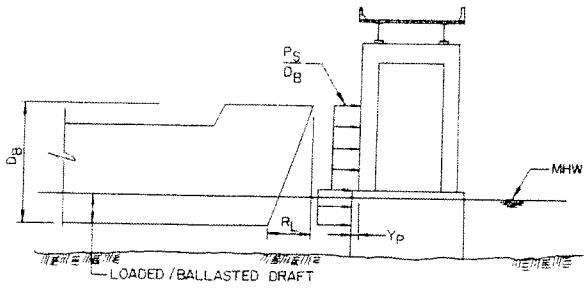

Figure 3.14.14.1-2 Ship Impact Line Load on Pier.

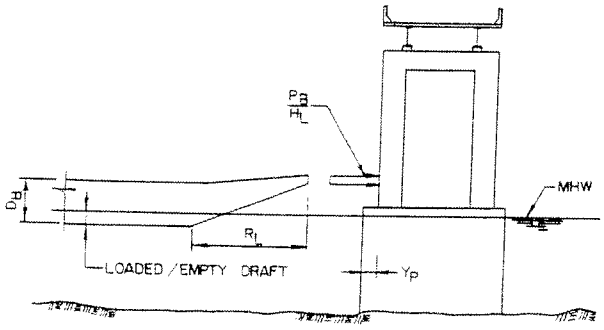

Figure 3.14.14.1-3 Barge Impact Force on Pier.

3.14.14.2 Superstructure Design

For superstructure design, the design impact force shall be applied as an equivalent static force transverse to the superstructure component in a direction parallel to the alignment of the centerline of the navigable channel.

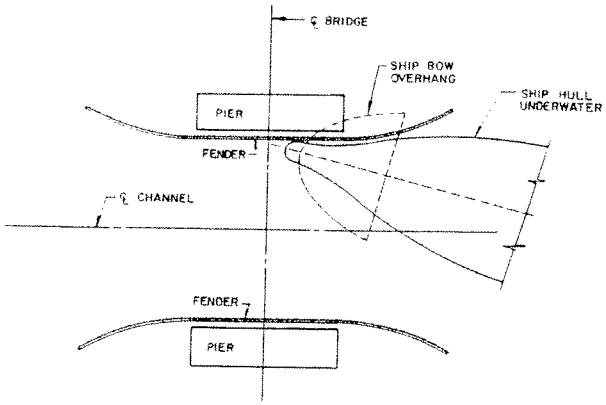

Figure C3.14.14.1-1 Plan of Ship Bow Overhang Impacting Pier.

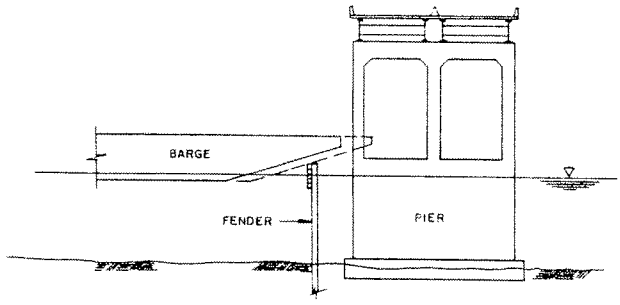

Figure C3.14.14.1-2 Elevation of Barge Bow Impacting Pier.

C3.14.14.2

The ability of various portions of a ship or barge to impact a superstructure component depends on the available vertical clearance under the structure, the water depth, vessel-type and characteristics, and the loading condition of the vessel.

3.14.15 Protection of Substructures

Protection may be provided to reduce or to eliminate the exposure of bridge substructures to vessel collision by physical protection systems, including fenders, pile cluster, pile-supported structures, dolphins, islands, and combinations thereof.

Severe damage and/or collapse of the protection system may be permitted, provided that the protection system stops the vessel prior to contact with the pier or redirects the vessel away from the pier.

C3.14.15

The development of bridge protection alternatives for vessel collisions generally follows three approaches:

- Reducing the annual frequency of collision events, for example, by improving navigation aids near a bridge;
- Reducing the probability of collapse, for example, by imposing vessel speed restrictions in the waterway; or
- Reducing the disruption costs of a collision, for example, by physical protection and motorist warning systems.

Because modifications to navigation aids in the waterway and vessel operating conditions are normally beyond the Bridge Designer's ability to implement, the primary area of bridge protection to be considered by the Designer are physical protection and motorist warning systems.

The current practice in the design of protective structures is almost invariably based on energy considerations. It is assumed that the loss of kinetic energy of the vessel is transformed into an equal amount of energy absorbed by the protective structure. The kinetic impact energy is dissipated by the work done by flexure, shear, torsion, and displacement of the components of the protective system.

Design of a protective system is usually an iterative process in which a trial configuration of a protective system is initially developed. For the trial, a force versus deflection diagram is developed via analysis or physical modeling and testing. The area under the diagram is the energy capacity of the protective system. The forces and energy capacity of the protective system is then compared with the design vessel impact force and energy to see if the vessel loads have been safely resisted.

REFERENCES

AASHTO. 1991. *Guide Specification and Commentary for Vessel Collision Design of Highway Bridges*, GVCB-1. American Association of State Highway and Transportation Officials, Washington, DC.

AASHTO. 2002. *Standard Specifications for Highway Bridges*, 17th Edition, HB-17. American Association of State Highway and Transportation Officials, Washington, DC.

AASHTO. 2004. *A Policy on Geometric Design of Highways and Streets,* GDHS-5. American Association of State Highway and Transportation Officials, Washington, DC.

Afanas'ev, V. P., Y. V. Dolgopolov, and I. Shyaishstein. 1971. "Ice Pressure on Individual Marine Structures." In *Ice Physics and Ice Engineering.* G. N. Yakocev, ed. Translated from the Russian by Israel Program for Scientific Translations, Jerusalem, Israel.

Allen, T. M. 2005. *Development of Geotechnical Resistance Factors and Downdrag Load Factors for LRFD Foundation Strength Limit State Design.* Publication No. FHWA-NHI-05-052. Federal Highway Administration, Washington, DC.

Allen, T. M., A. Nowak, and R. Bathurst. 2005. *Calibration to Determine Load and Resistance Factors for Geotechnical and Structural Design.* TRB Circular E-C079, Transportation Research Board, Washington, DC.

ASCE. 1980. "Loads and Forces on Bridges." *Preprint 80-173.* American Society of Civil Engineers National Convention, Portland, OR, April 14–18, 1980.

ASCE. 1988. *Minimum Design Loads for Building and Other Structures*, ASCE 7-88. American Society of Civil Engineers, New York, NY.

AUSTROADS. 1992. *Bridge Design Code.* Hay Market, Australia.

Briaud, J. and L. Tucker. 1993. *Downdrag on Bitumen-Coated Piles*, NCHRP 393/Project 24-05, Transportation Research Board, National Research Council, Washington, DC.

Burg, R. G. and A.E. Fiorato. 1999. "High-Strength Concrete in Massive Foundation Elements." *PCA Research and Development Bulletin RD117.* Portland Cement Association, Skokie, IL.

Burg, R. G. and B.W. Ost. 1992. "Engineering Properties of Commercially Available High-Strength Concretes." *PCA Research and Development Bulletin RD104T.* Portland Cement Association, Skokie, IL.

Caquot, A., and J. Kerisel. 1948. *Tables for the Calculation of Passive Pressure, Active Pressure and Bearing Capacity of Foundations.* Gauthier-Villars, Libraire du Bureau des Longitudes, de L'Ecole Polytechnique, Paris.

CBA/Buckland and Taylor. 1982. "Annacis Island Bridge." In Report No. 3, *Ship Collision Risk Analysis.* Prepared for the British Columbia Ministry of Transportation and Highways, July 1982.

Cheney, R. S. 1984. "Permanent Ground Anchors." FHWA-DP-68-1R Demonstration Project. FHWA, U.S. Department of Transportation, Washington, DC, p. 132.

Cheney, R. S. and R. Chassie. 2000. *Soils and Foundations Workshop Reference Manual*, NHI-00-045. National Highway Institute, Federal Highway Administration, U.S. Department of Transportation, Washington, DC.

Clausen, C. J. F., and S. Johansen. 1972. "Earth Pressures Measured Against a Section of a Basement Wall," *Proceedings, 5th European Conference on SMFE.* Madrid, Spain, pp. 515–516.

Clough, G. W., and J. M. Duncan. 1991. "Earth Pressures." *Foundation Engineering Handbook*, 2nd Edition. H. Y. Fang, ed. Van Nostrand Reinhold, New York, NY, Chap. 6.

Clough, G. W., and T. D. O'Rourke. 1990. "Construction-Induced Movements of In-Situ Walls." In *Proc. of the 1990 Specialty Conference on Design and Performance of Earth Retaining Structures.* Ithaca, NY, pp. 439–470.

Clough, G. W., and Y. Tsui. 1974. "Performance of Tied-Back Retaining Walls." *Journal of the Geotechnical Engineering Division*, American Society of Civil Engineers, New York, NY, Vol. 100, No. GT 12, pp. 1259–1273.

Coastal Engineering Research Center. 1984. *Shore Protection Manual*, 4th Edition. Coastal Engineering Research Center, Washington, DC.

Cohen, H. 1990. *Truck Weight Limits: Issues and Options*, Special Report 225. Transportation Research Board, National Research Council, Washington, DC.

Cowiconsult, Inc. 1981. *Sunshine Skyway Bridge Ship Collision Risk Assessment*. Prepared for Figg and Muller Engineers, Inc., Lyngby, Denmark, September 1981.

Cowiconsult. 1987. "General Principles for Risk Evaluation of Ship Collisions, Strandings, and Contact Incidents." Technical note, January 1987.

CSA. 2000. *Canadian Highway Bridge Design Code*, CAN/CSA-S6-00. Canadian Standards Association International, Section 3, Loads, Toronto, ON.

CSA. 1988. *Design of Highway Bridges*, CAN/CSA-S6-88. Canadian Standards Association, Rexdale, ON.

Csagoly, P. F., and Z. Knobel. 1981. *The 1979 Survey of Commercial Vehicle Weights in Ontario*. Ontario Ministry of Transportation and Communications, Toronto, ON.

D'Appolonia, E. 1999. *Developing New AASHTO LRFD Specifications for Retaining Walls*, Report for NCHRP Project 20-7, Task 88, Transportation Research Board, National Research Council, Washington, DC.

FHWA. 2001. "Highway Performance Concrete." Compact Disc, Federal Highway Administration, U.S. Department of Transportation, August 2001.

Flaate, K. S. 1966. *Stresses and Movements in Connection with Braced Cuts in Sand and Clay*. Ph.D Dissertation, University of Illinois, Urbana, IL.

Fujii, Y. and R. Shiobara. 1978. "The Estimation of Losses Resulting from Marine Accidents." *Journal of Navigation*, Cambridge University Press, Cambridge, England, Vol. 31, No. 1.

Gajer, R. B., and V. P. Wagh. 1994. "Bridge Design for Seismic Performance Category B: The Problem with Foundation Design," *Proceeding No. 11th International Bridge Conference,* Paper IBC-94-62, Pittsburgh, PA.

Gerard, R., and S. J. Stanely. 1992. "Probability Analysis of Historical Ice Jam Data for a Complex Reach: A Case Study." *Canadian Journal of Civil Engineering*, NRC Research Press, Ottawa, ON.

Hanna, T. H., and G. A. Matallana. 1970. "The Behavior of Tied-Back Retaining Walls." *Canadian Geotechnical Journal*, NRC Research Press, Ottawa, ON, Vol. 7, No. 4, pp. 372–396.

Hannigan, P. J., G. G. Goble, G. Thendean, G. E. Likins, and F. Rausche. 2005. *Design and Construction of Driven Pile Foundations*, Vol. I and II. Federal Highway Administration Report No. FHWA-HI-05. Federal Highway Administration, Washington, DC.

Haynes, F. D. 1995. *Bridge Pier Design for Ice Forces*. Ice Engineering, U.S. Army Cold Regions Research and Engineering Laboratory, Hanover, NH.

Haynes, F. D. 1996. Private communications.

Highway Engineering Division. 1991. *Ontario Highway Bridge Design Code*, 3rd Edition. Highway Engineering Division, Ministry of Transportation and Communications, Toronto, ON.

Hirsch, T. J. 1989. *Analysis and Design of Metrorail-Railroad Barrier Systems*. Texas A&M University, College Station, TX.

Holtz, R. D., and W. D. Kovacs. 1981. *An Introduction to Geotechnical Engineering*, Prentice-Hall, Inc., Englewood Cliffs, NJ.

Huiskamp, W. J. 1983. *Ice Force Measurements on Bridge Piers, 1980–1982*, Report No. SWE 83-1. Alberta Research Council, Edmonton, AB.

Imbsen, R. A., D. E. Vandershaf, R. A. Schamber, and R. V. Nutt. 1985. *Thermal Effects in Concrete Bridge Superstructures*, NCHRP Report 276. Transportation Research Board, National Research Council, Washington, DC.

International Association of Bridge and Structural Engineers. 1983. "Ship Collision with Bridges and Offshore Structures." In *International Association of Bridge and Structural Engineers Colloquium*, Copenhagen, Denmark. 3 vols.

Ishihara, K. and M. Yoshimine. 1992. "Evaluation of Settlements in Sand Deposits Following Liquefaction during Earthquakes." *Soils and Foundations,* JSSMFE, Vol. 32, No. 1, March, pp. 173–188.

Kavazanjian, E., Jr., N. Matasoviæ, T. Hadj-Hamou, and P. J. Sabatini. 1997. *Design Guidance: Geotechnical Earthquake Engineering for Highways*. Geotechnical Engineering Circular No. 3, Report No. FHWA-SA-97-076. Federal Highway Administration, U.S. Department of Transportation, Washington, DC.

Knott, J., D. Wood, and D. Bonyun. 1985. "Risk Analysis for Ship-Bridge Collisions." *Fourth Symposium on Coastal and Ocean Management*. American Society of Civil Engineers, Baltimore, MD, July 30–August 2, 1985.

Kulicki, J. M., and D. R. Mertz. 1991. "A New Live Load Model for Bridge Design." In *Proc. of the 8th Annual International Bridge Conference*, June 1991, pp. 238–246.

Larsen, D. D. 1983. "Ship Collision Risk Assessment for Bridges." In Vol. 1, *International Association of Bridge and Structural Engineers Colloquium*. Copenhagen, Denmark, pp. 113–128.

Larsen, O. D. 1993. "Ship Collision with Bridges—The Interaction Between Vessel Traffic and Bridge Structures." *IABSE Structural Engineering Document 4*, IABSE-AIPC-IVBH, Zürich, Switzerland.

Lipsett, A. W., and R. Gerard. 1980. *Field Measurement of Ice Forces on Bridge Piers 1973–1979*, Report SWE 80-3. Alberta Research Council, Edmonton, AB.

Liu, H. 1991. *Wind Engineering: A Handbook for Structural Engineers*, Prentice Hall, Englewood Cliffs, NJ.

Mander, J. B., M. J. N. Priestley, and R. Park. 1988. "Observed Stress-Strain Behavior of Confined Concrete." *Journal of the Structural Division*, American Society of Civil Engineers, New York, NY, August 1988.

Mander, J. B., M. J. N. Priestley, and R. Park. 1988. "Theoretical Stress-Strain Model for Confined Concrete." *Journal of the Structural Division*, American Society of Civil Engineers, New York, NY, August 1988.

Meir-Dornberg, K. E. 1983. "Ship Collisions, Safety Zones, and Loading Assumptions for Structures on Inland Waterways." *VDI-Berichte*, No. 496, pp. 1–9.

Modjeski and Masters, Consulting Engineers. 1984. *Criteria for the Design of Bridge Piers with Respect to Vessel Collision in Louisiana Waterways*. Prepared for the Louisiana Department of Transportation and Development and the Federal Highway Administration, Harrisburg, PA, November 1984.

Montgomery, C. T., R. Gerard, W. J. Huiskamp, and R. W. Kornelsen. 1984. "Application of Ice Engineering to Bridge Design Standards." In *Proc., Cold Regions Engineering Specialty Conference*. Canadian Society for Civil Engineering, Montreal, QC, April 4–6, 1984, pp. 795–810.

Montgomery, C. J., R. Gerard, and A. W. Lipsett. 1980. "Dynamic Response of Bridge Piers to Ice Forces." *Canadian Journal of Civil Engineering*, , NRC Research Press, Ottawa, ON, Vol. 7, No. 2, pp. 345–356.

Montgomery, C. J., and A. W. Lipsett. 1980. "Dynamic Tests and Analysis of a Massive Pier Subjected to Ice Forces." *Canadian Journal of Civil Engineering*, , NRC Research Press, Ottawa, ON, Vol. 7, No. 3, pp. 432–441.

Neill, C. R. 1976. "Dynamic Ice Forces on Piers and Piles: An Assessment of Design Guidelines in the Light of Recent Research." *Canadian Journal of Civil Engineering*, , NRC Research Press, Ottawa, ON, Vol. 3, No. 2, pp. 305–341.

Neill, C. R., ed. 1981. *Ice Effects on Bridges*. Roads and Transportation Association of Canada, Ottawa, ON.

Nevel, D. E. 1972. "The Ultimate Failure of a Floating Ice Sheet." In *Proc., International Association for Hydraulic Research, Ice Symposium*, pp. 17–22.

Nicholson, P. J., D. D. Uranowski, and P. T. Wycliffe-Jones. 1981. *Permanent Ground Anchors: Nicholson Design Criteria*, FHWA/RD/81-151. Federal Highway Administration, U.S. Department of Transportation, Washington, DC, p. 151.

Nowak, A. S. 1992. *Calibration of LRFD Bridge Design Code*, NCHRP Project 12-33. University of Michigan, Ann Arbor, MI.

Nowak, A. S. 1995. "Calibration of LRFD Bridge Design Code." *Journal of Structural Engineering*, American Society of Civil Engineers, New York, NY, Vol. 121, No. 8, pp. 1245–1251.

Nowak, A. S. 1999. *Calibration of LRFD Bridge Design Code*. NCHRP Report 368, Transportation Research Board, National Research Council, Washington, DC.

O'Rourke, T. D. 1975. *A Study of Two Braced Excavations in Sand and Interbedded Stiff Clay*. Ph.D Dissertation, University of Illinois, Urbana, IL.

Page, J. 1976. *Dynamic Wheel Load Measurements on Motorway Bridges*. Transportation and Road Research Laboratory, Crowthorne, Berkshare, UK.

Paikowsky, S. G., with contributions from B. Birgisson, M. McVay, T. Nguyen, C. Kuo, G. Baecher, B. Ayyab, K. Stenersen, K. O'Malley, L. Chernauskas, and M. O'Neill. 2004. *Load and Resistance Factor Design (LRFD) for Deep Foundations*. NCHRP (Final) Report 507, Transportation Research Board, National Research Council, Washington, DC.

Peck, R. B., W. E. Hanson, and T. H. Thornburn. 1974. *Foundation Engineering*, 2nd Edition. John Wiley and Sons, Inc., New York, NY.

PIANC. 1984. *Report of the International Commission for Improving the Design of Fender Systems*. International Navagation Association, Brussels, Belgium.

Poulos, H. G., and E. H. Davis. 1974. *Elastic Solutions for Soil and Rock Mechanics*. John Wiley and Sons, Inc., New York, NY.

Priestley, M. J. N., R. Parks, and R. T. Potangaroa. 1981. "Ductility of Spirally Confined Concrete Columns." *Journal of the Structural Division*, American Society of Civil Engineers, New York, NY, January 1981.

Priestley, M. J. N., F. Seible and G. M. Calvi. 1996. *Seismic Design and Retrofit of Bridges*. John Wiley and Sons, Inc., New York, NY.

Priestley, M. J. N., F. Seible, and Y. H. Chai. 1992. "Design Guidelines for Assessment Retrofit and Repair of Bridges for Seismic Performance." University of California, San Diego, CA.

Prucz, Z., and W. B. Conway. 1987. "Design of Bridge Piers Against Ship Collision." *Bridges and Transmission Line Structures*. L. Tall, ed: American Society of Civil Engineers, New York, NY, pp. 209–223.

Ritter, M. A. 1990. *Timber Bridges: Design, Construction, Inspection, and Maintenance*, EM7700-B. Forest Service, U.S. Department of Agriculture, Washington, DC.

Roeder, C. W. 2002. *Thermal Design Procedure for Steel and Concrete Bridges*. Final Report for NCHRP 20-07/106. Transportation Research Board, National Research Council, Washington, D.C., April 2002.

Rowe, W. D. 1977. *An Anatomy of Risk*. John Wiley and Sons, Inc., New York, NY.

Sabatini, P. J., D. G. Pass, and R. C. Bachus. 1999. *Geotechnical Engineering Circular No. 4—Ground Anchors and Anchored Systems*, Federal Highway Administration, Report No. FHWA-SA-99-015. NTIS, Springfield, VA.

Saul, R. and H. Svensson. 1980. "On the Theory of Ship Collision Against Bridge Piers." In *IABSE Proceedings*, February 1980, pp. 51–82.

Schnabel, Jr., H. 1982. *Tiebacks in Foundation Engineering and Construction*. McGraw-Hill, New York, NY, p. 171.

Sherif, M. A., I. Ishibashi, and C. D. Lee. 1982. "Earth Pressures Against Rigid Retaining Walls." *Journal of Geotechnical Engineering Division*, American Society of Civil Engineers, New York, NY, Vol. 108, GT5, pp. 679–695.

Simiu, E. 1973. "Logarithmic Profiles and Design Wind Speeds." *Journal of the Mechanics Division*, American Society of Civil Engineers, New York, NY, Vol. 99, No. EM5, October 1973, pp. 1073–1083.

Simiu, E. 1976. "Equivalent Static Wind Loads for Tall Building Design." *Journal of the Structures Division*, American Society of Civil Engineers, New York, NY, Vol. 102, No. ST4, April, 1976, pp. 719–737.

Terzaghi, K. 1934. "Retaining Wall Design for Fifteen-Mile Falls Dam." *Engineering News Record*, May 1934, pp. 632 –636.

Terzaghi, K., and R. B. Peck. 1967. *Soil Mechanics in Engineering Practice*, 2nd Edition. John Wiley and Sons, Inc., New York, NY, p. 729.

Tokimatsu, K. and B. Bolton Seed. 1987. Evaluation of Settlements in Sands due to Earthquake Shaking. *Journal of Geotechnical Engineering*. American Society of Civil Engineers, Vol. 113, No. 8, pp. 861–878.

Transit New Zealand. 1991. *Bridge Manual: Design and Evaluation*. Draft. Transit New Zealand, Wellington, New Zealand.

U.S. Department of the Navy. 1982. *Foundations and Earth Structures*, Technical Report NAVFAC DM-7.1 and DM-7.2. Naval Facilities Command, U.S. Department of Defense, Washington, DC, p. 244.

U.S. Department of the Navy. 1982. "Soil Mechanics." *Design Manual 7.1,* NAVFAC DM-7.1. Naval Facilities Engineering Command, U.S. Department of Defense, Alexandria, VA, p. 348.

Whitman, R.V. 1984. "Evaluating Calculated Risk in Geotechnical Engineering." *Journal of Geotechnical Engineering*, American Society of Civil Engineers, New York, NY, Vol. 110, No. 2, February 1984, pp. 145–188.

Williams, G. P. 1963. "Probability Charts for Predicting Ice Thickness." *Engineering Journal*, June 1963, pp. 3–7.

Woisin, G. 1976. "The Collision Tests of the GKSS." In *Jahrbuch der Schiffbautechnischen Gesellschaft*, Vol. 70. Berlin, Germany, pp. 465–487.

Zabilansky, L. J. 1996. "Ice Force and Scour Instrumentation for the White River, Vermont." *Special Report 96-6*. U.S. Army Cold Regions Research and Engineering Laboratory, U.S. Department of Defense, Hanover, NH.

APPENDIX A3 SEISMIC DESIGN FLOWCHARTS

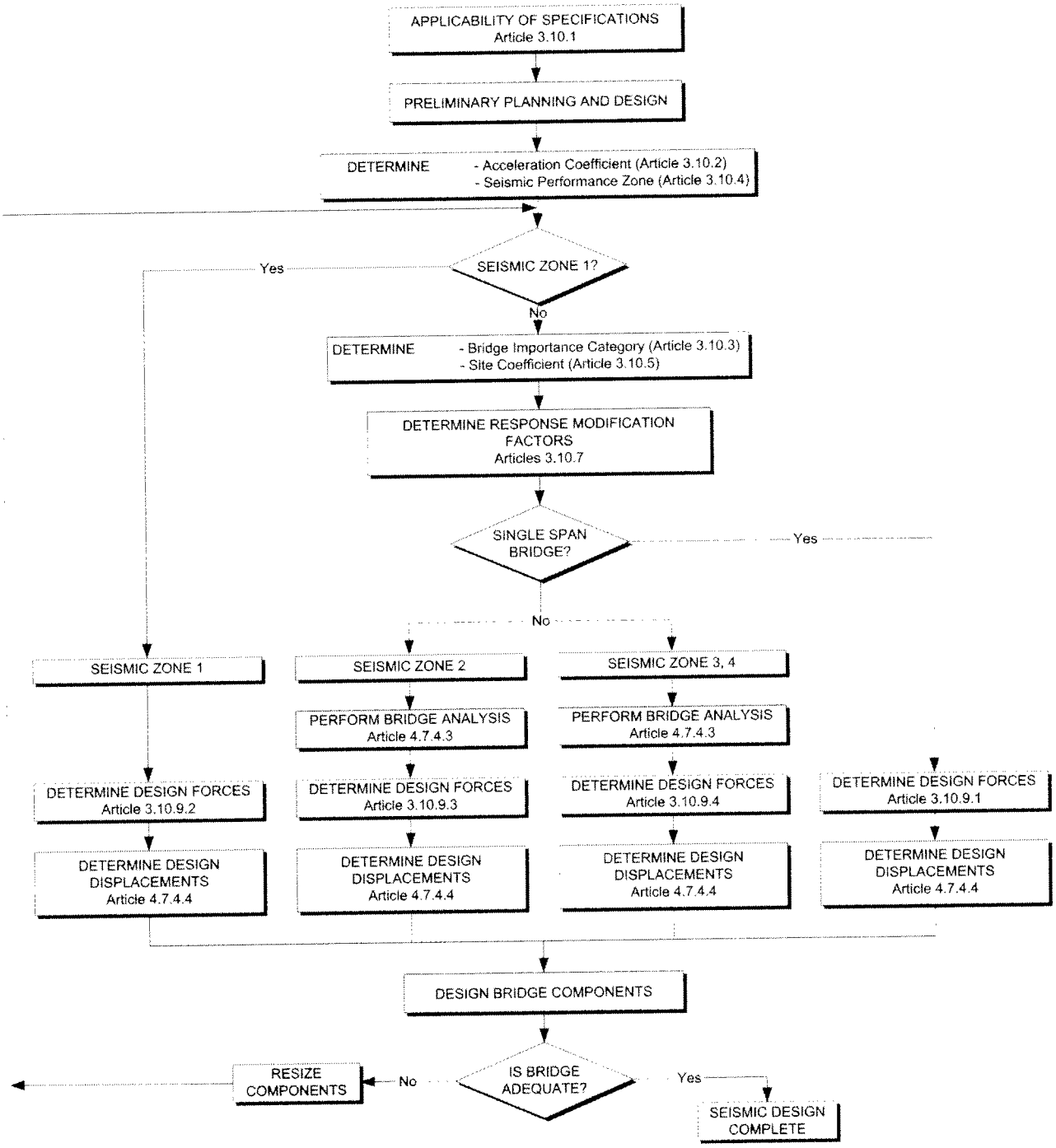

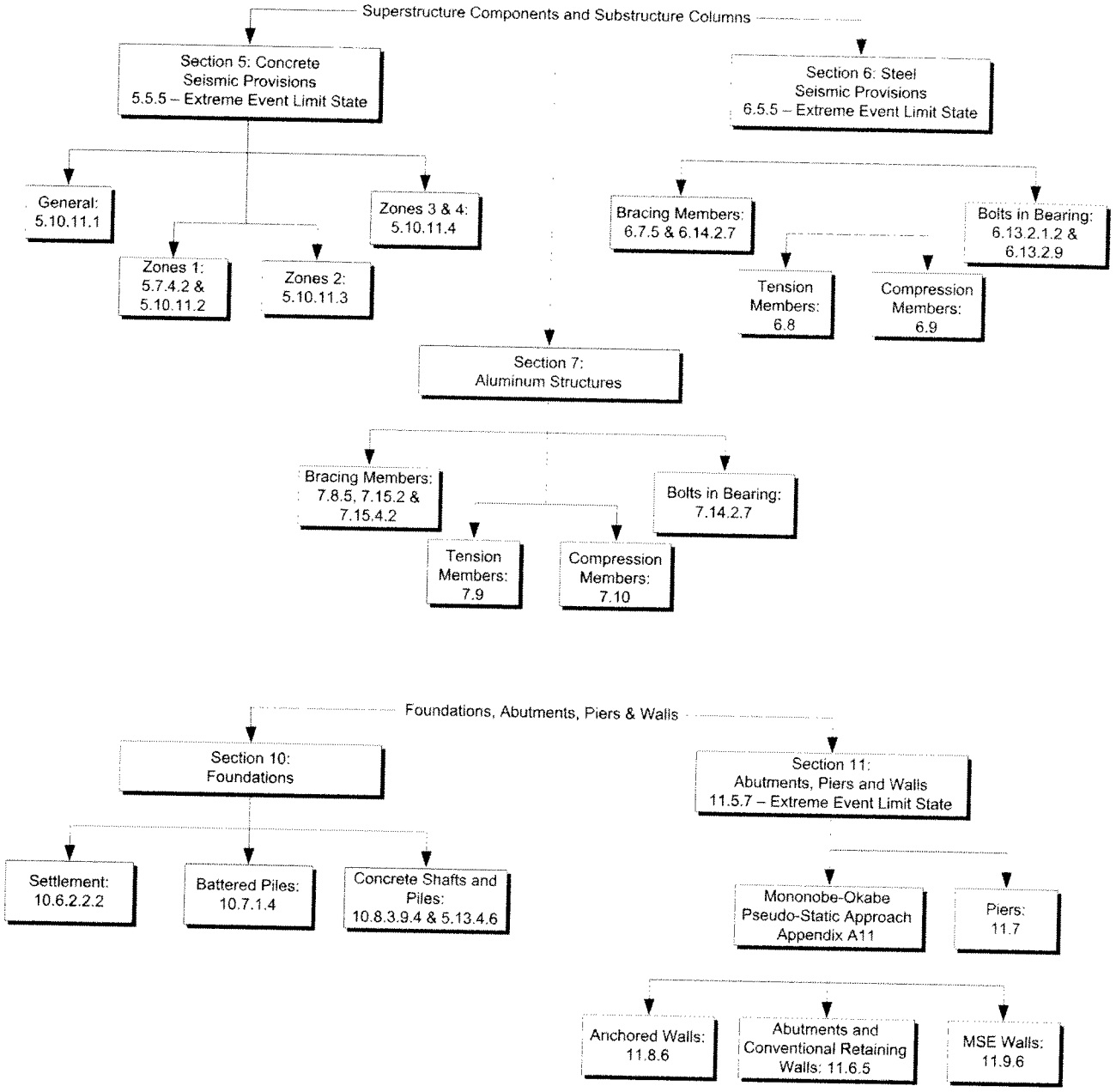
Superstructure Components and Substructure Columns
Section 5: Concrete Seismic Provisions 5.5.5 – Extreme Event Limit State
Section 6: Steel Seismic Provisions 6.5.5 – Extreme Event Limit State
General: 5.10.11.1
Zones 1: 5.7.4.2 & 5.10.11.2
Zones 2: 5.10.11.3
Zones 3 & 4: 5.10.11.4
Bracing Members: 6.7.5 & 6.14.2.7
Tension Members: 6.8
Compression Members: 6.9
Bolts in Bearing: 6.13.2.1.2 & 6.13.2.9
Section 7: Aluminum Structures
Bracing Members: 7.8.5, 7.15.2 & 7.15.4.2
Tension Members: 7.9
Compression Members: 7.10
Bolts in Bearing: 7.14.2.7
Foundations, Abutments, Piers & Walls
Section 10: Foundations
Settlement: 10.6.2.2.2
Battered Piles: 10.7.1.4
Concrete Shafts and Piles: 10.8.3.9.4 & 5.13.4.6
Section 11: Abutments, Piers and Walls 11.5.7 – Extreme Event Limit State
Mononobe-Okabe Pseudo-Static Approach Appendix A11
Piers: 11.7
Anchored Walls: 11.8.6
Abutments and Conventional Retaining Walls: 11.6.5
MSE Walls: 11.9.6

APPENDIX B3 OVERSTRENGTH RESISTANCE

Article 3.10.9.4.3a defines the forces resulting from plastic hinging, i.e., a column reaching its ultimate moment capacity, in the columns and presents two procedures. One is for a single column hinging about its two principal axes; this is also applicable for piers and bents acting as single columns. The other procedure is for a multiple column bent in the plane of the bent. The forces are based on the potential overstrength resistance of the materials, and to be valid the design detail requirements of this section must be used so that plastic hinging of the columns can occur. The overstrength resistance results from actual properties being greater than the minimum specified values and is implemented by specifying resistance factors greater than unity. This fact must be accounted for when forces generated by yielding of the column are used as design forces. Generally, overstrength resistance depends on the following factors:

- The actual size of the column and the actual amount of reinforcing steel.
- The effect of an increased steel strength over the specified f_y and for strain hardening effects.
- The effect of an increased concrete strength over the specified f'_c and confinement provided by the transverse steel. Also, with time, concrete will gradually increase in strength.
- The effect of an actual concrete ultimate compressive strain above 0.003.

Column Size and Reinforcement Configuration

The design engineer should select the minimum column section size and steel reinforcement ratio when satisfying structural design requirements. As these parameters increase, the overstrength resistance increases. This may lead to an increase in the foundation size and cost. A size and reinforcement ratio which forces the design below the nose of the interaction curve is preferable, especially in high seismic areas. However, the selection of size and reinforcement must also satisfy architectural, and perhaps other requirements, which may govern the design.

Increase in Reinforcement Strength

Almost all reinforcing bars will have a yield strength larger than the minimum specified value which may be up to 30 percent higher, with an average increase of 12 percent. Combining this increase with the effect of strain hardening, it is realistic to assume an increased yield strength of $1.25 f_y$, when computing the column overstrength.

Increase in Concrete Strength

Concrete strength is defined as the specified 28-day compression strength; this is a low estimate of the strength expected in the field. Typically, conservative concrete batch designs result in actual 28-day strengths of about 20 to 25 percent higher than specified. Concrete will also continue to gain strength with age. Tests on cores taken from older California bridges built in the 1950s and 1960s have consistently yielded compression strength in excess of $1.5 f'_c$. Concrete compression strength is further enhanced by the possible confinement provided by the transverse reinforcement. Rapid loading due to seismic forces could also result in significant increase in strength, i.e., strain rate effect. In view of all the above, the actual concrete strength when a seismic event occurs is likely to significantly exceed the specified 28-day strength. Therefore, an increased concrete strength of $1.5 f'_c$ could be assumed in the calculation of the column overstrength resistance.

Ultimate Compressive Strain (ε_c)

Although tests on unconfined concrete show 0.003 to be a reasonable strain at first crushing, tests on confined column sections show a marked increase in this value. The use of such a low extreme fiber strain is a very conservative estimate of strains at which crushing and spalling first develop in most columns, and considerably less than the expected strain at maximum response to the design seismic event. Research has supported strains on the order of 0.01 and higher as the likely magnitude of ultimate compressive strain. Therefore, designers could assume a value of ultimate strain equal to 0.01 as a realistic value.

For calculation purposes, the thickness of clear concrete cover used to compute the section overstrength shall not be taken to be greater than 2.0 in. This reduced section shall be adequate for all applied loads associated with the plastic hinge.

Overstrength Capacity

The derivation of the column overstrength capacity is depicted in Figure B3-1. The effect of higher material properties than specified is illustrated by comparing the actual overstrength curve, computed with realistic f'_c, f_y and ε_c values, to the nominal strength interaction curve, P_n, M_n. It is generally satisfactory to approximate the overstrength capacity curve by multiplying the nominal moment strength by the 1.3 factor for axial loads below the nose of the interaction curve, i.e., P_n, 1.3 M_n curve. However, as shown, this curve may be in considerable error for axial loads above the nose of the interaction curve. Therefore, it is recommended that the approximate overstrength curve be obtained by multiplying both P_n and M_n by $\phi = 1.3$, i.e., 1.3 P_n, 1.3 M_n. This curve follows the general shape of the actual curve very closely at all levels of axial loads.

In the light of the above discussion, it is recommended that:

- For all bridges with axial loads below P_b, the overstrength moment capacity shall be assumed to be 1.3 times the nominal moment capacity.
- For bridges in Zones 3 and 4 with **operational** classification of "other", and for all bridges in Zone 2 for which plastic hinging has been invoked, the overstrength curve for axial loads greater than P_b shall be approximated by multiplying both P_n and M_n by $\phi = 1.3$.
- For bridges in Zones 3 and 4 with **operational** classification of "essential" or "critical", the overstrength curve for axial loads greater than P_b shall be computed using realistic values for f'_c, f_y and ε_c as recommended in Table B3-1 or from values based on actual test results. The column overstrength, thus calculated, should not be less than the value estimated by the approximate curve based on 1.3 P_n, 1.3 M_n.

Table B3-1 Recommended Increased Values of Materials Properties.

Increased f_y (minimum)	1.25 f_y
Increased f'_c	1.5 f'_c
Increased ε_c	0.01

Shear Failure

The shear mode of failure in a column or pile bent will probably result in a partial or total collapse of the bridge; therefore, the design shear force must be calculated conservatively. In calculating the column or pile bent shear force, consideration must be given to the potential locations of plastic hinges. For flared columns, these may occur at the top and bottom of the flare. For multiple column bents with a partial-height wall, the plastic hinges will probably occur at the top of the wall unless the wall is structurally separated from the column. For columns with deeply embedded foundations, the plastic hinge may occur above the foundation mat or pile cap. For pile bents, the plastic hinge may occur above the calculated point of fixity. Because of the consequences of a shear failure, it is recommended that conservatism be used in locating possible plastic hinges such that the smallest potential column length be used with the plastic moments to calculate the largest potential shear force for design.

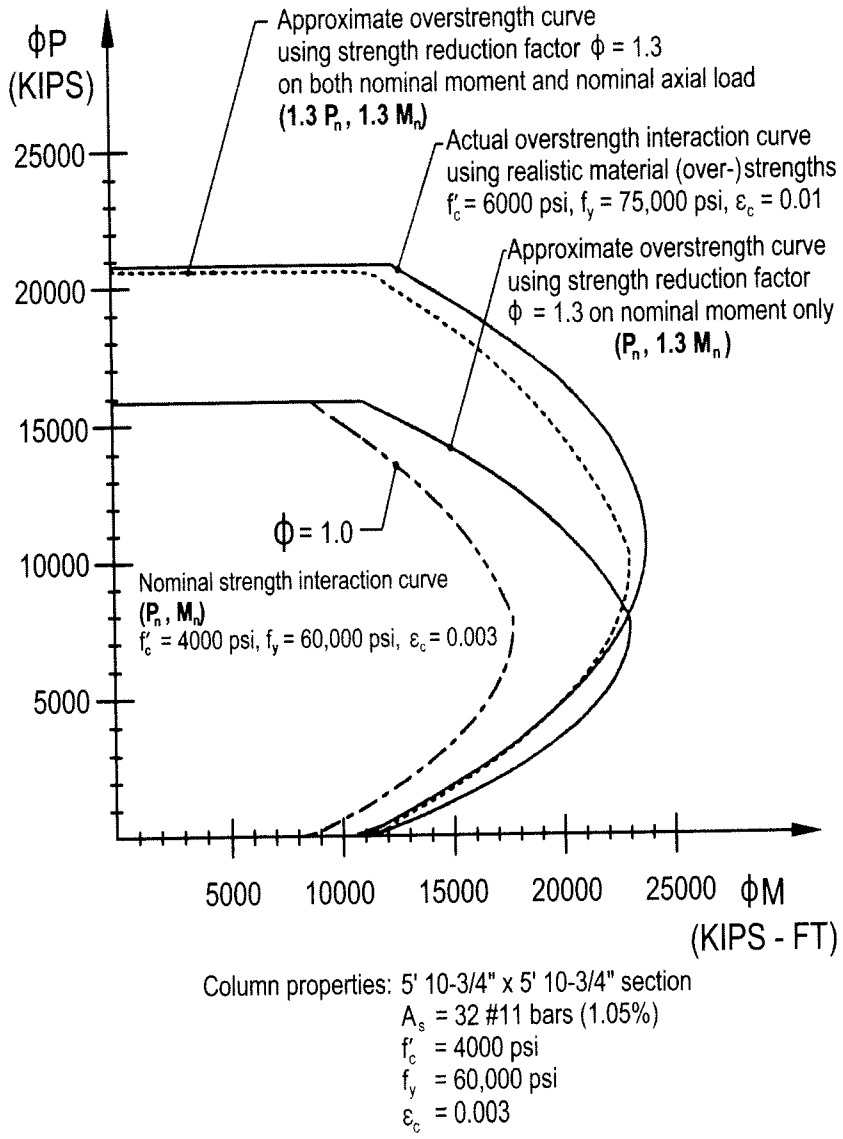

Figure B3-1 Development of Approximate Overstrength Interaction Curves from Nominal Strength Curves after Gajer and Wagh (*1994*).